OXYGEN ISOTOPES AND TRACE ELEMENTS IN THE TIVA CANYON TUFF, YUCCA MOUNTAIN AND VICINITY, NYE COUNTY, NEVADA

USGS-OFR--95-431

U.S. GEOLOGICAL SURVEY

Open-File Report 95-431

MASTER

Oxygen Isotopes and Trace Elements in the Tiva Canyon Tuff, Yucca Mountain and Vicinity, Nye County, Nevada

by Brian D. Marshall, T. Kurtis Kyser, and Zell E. Peterman

U.S. GEOLOGICAL SURVEY

Open-File Report 95-431

MASTER

Denver, Colorado
1996

U.S. DEPARTMENT OF THE INTERIOR
BRUCE BABBITT, Secretary

U.S. GEOLOGICAL SURVEY
Gordon P. Eaton, Director

CONTENTS

FIGURES

TABLES

CONVERSION FACTORS AND VERTICAL DATUM

Multiply	By	To obtain
millimeter (mm)	0.03937	inch
meter (m)	3.2808	foot
kilometer (km)	0.6214	mile
kilogram (kg)	2.2046	pound

Sea level: In this report "sea level" refers to the National Geodetic Vertical Datum of 1929 (NGVD of 1929)—a geodetic datum derived from a general adjustment of the first-order level nets of both the United States and Canada, formerly called Sea Level Datum of 1929.

Oxygen Isotopes and Trace Elements in the Tiva Canyon Tuff, Yucca Mountain and Vicinity, Nye County, Nevada

By Brian D. Marshall, T. Kurtis Kyser, and Zell E. Peterman

Abstract

Yucca Mountain, located in Nye County, Nevada, is being studied as a potential site for an underground repository for high-level radioactive waste. Because Yucca Mountain is located in a resource-rich geologic setting, one aspect of the site characterization studies is an evaluation of the resource potential at Yucca Mountain.

The Tiva Canyon Tuff is a widespread felsic ash-flow sheet that is well exposed in the Yucca Mountain area. Samples of the upper part of the Tiva Canyon Tuff were selected to evaluate the potential for economic mineral deposits within the Miocene volcanic section. These samples of the upper cliff and caprock subunits have been analyzed for oxygen isotopes and a large suite of elements. Oxygen isotope compositions ($\delta^{18}O$) of the Tiva Canyon Tuff are typical of felsic igneous rocks but range from 6.9 to 11.8 permil, indicating some post-depositional alteration. There is no evidence of the low $\delta^{18}O$ values (less than 6 permil) that are typical of epithermal precious-metal deposits in the region. The variation in oxygen isotope ratios is probably the result of deuteric alteration during late-stage crystallization of silica and low-temperature hydration of glassy horizons; these processes are also recorded by the chemical compositions of the rocks. However, most elemental contents in the Tiva Canyon Tuff reflect igneous processes, and the effects of alteration are observed only in some of the more mobile elements.

These studies indicate that the Tiva Canyon Tuff at Yucca Mountain has not been affected by large-scale meteoric-water hydrothermal circulation. The chemical compositions of the Tiva Canyon Tuff, especially the low concentrations of most trace elements including typical pathfinder elements, show no evidence for epithermal metal deposits. Together, these data indicate that the potential for economic mineralization in this part of the volcanic section at Yucca Mountain is small.

INTRODUCTION

Yucca Mountain in Nye County in southern Nevada (fig. 1) is being evaluated as a site for the construction of a potential high-level nuclear waste repository (U.S. Department of Energy, 1988). Yucca Mountain is located in the resource-rich geologic environment of the Basin and Range Province, which has substantial precious-metal production and hydrocarbon and geothermal potential (Ransome, 1907; 1910; Cornwall, 1972; Castor and others, 1990; Grow and others, 1994). Indications of naturally occurring materials or energy sources that would attract exploration and development are potentially adverse conditions (Younker and others, 1992) for a nuclear waste storage site. Thus, a careful assessment of the resource potential of Yucca Mountain is essential for evaluating the suitability of the site. This work is being carried out under the Human Interference Program described in the Site Characterization Plan (U.S. Department of Energy, 1988, Section 8.3.1.9, p. 1–55).

This report describes a geochemical and isotopic study of outcrop samples of the Tiva Canyon Tuff from the conceptual controlled area (fig. 2). The study
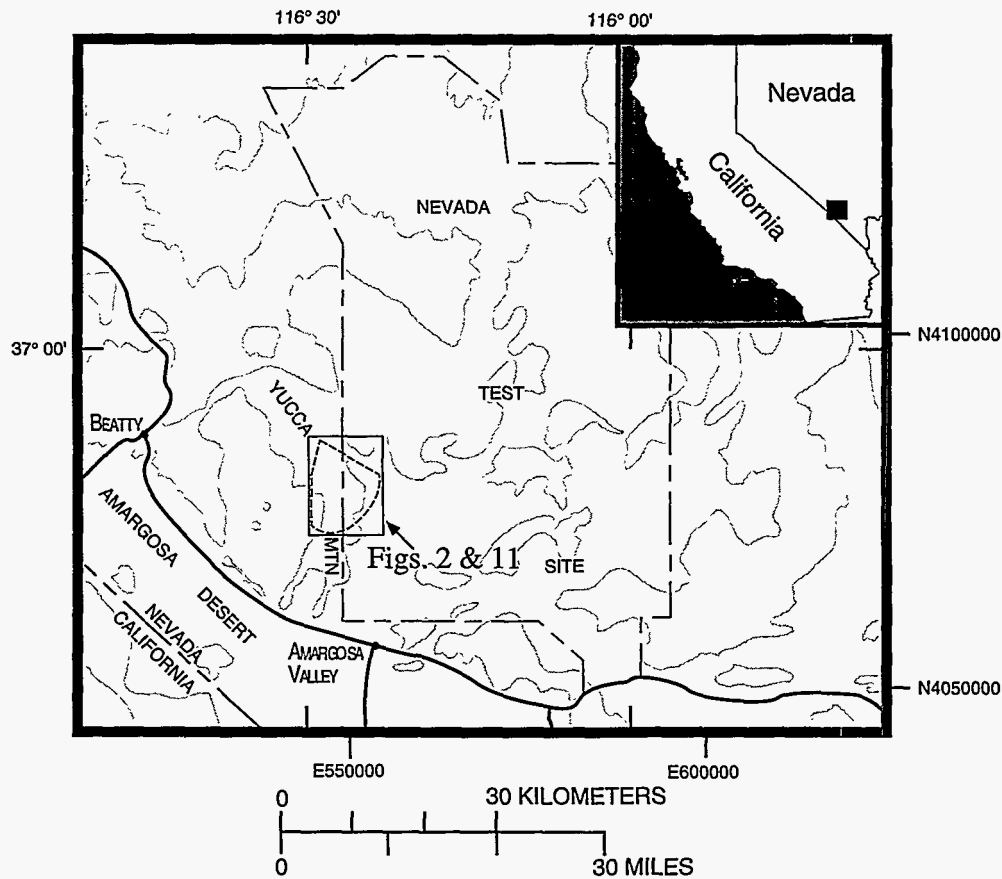
Figure 1. Southern Nevada and location of the Nevada Test Site and the areas shown on figures 2 and 11.

was designed to detect subtle indications of past interactions of the Tiva Canyon Tuff with hydrothermal solutions (heated meteoric waters). Such evidence of intermediate- to high-temperature water-rock interaction may indicate the possibility that mineral deposits may be present in the volcanic rock mass within and beneath the Tiva Canyon Tuff. Previous studies by the U.S. Geological Survey that were related to assessment of mineral resources include: (1) a synthesis of known mineral occurrences (Bergquist and McKee, U.S. Geological Survey, written commun., 1991), (2) an evaluation of the hydrocarbon potential (Grow and others, 1994), (3) the development of isotopic techniques for identifying potentially mineralized Paleozoic limestones (Peterman and others, 1994), and (4) an evaluation of the effects of hydrothermal activity along potential fluid pathways in the volcanic rocks (Neymark and others, 1995). These studies all suggest a low potential for economic resources at Yucca Mountain.

Geologic Description of Study Area

Yucca Mountain is composed of a thick sequence (up to 1,300 m) of late Tertiary felsic ash-flow tuffs that were deposited on a basement of Paleozoic carbonate rocks (Spengler and Fox, 1989). Host rocks for potential hydrothermal mineralization include the volcanic rocks of the Paintbrush Group, the underlying Crater Flat Group and older volcanic units that are generally altered to zeolites and other secondary minerals, and Paleozoic and Late Proterozoic sedimentary rocks. In the Basin and Range Province, all of these rock types are known to host both disseminated and vein-type precious-metal deposits (Romberger, 1988, 1993). Within a few tens of kilometers of Yucca Mountain, all of these same rock sequences host precious-metal deposits (Bergquist and McKee, U.S. Geological Survey, written commun., 1991; Peterman and others, 1994; Weiss and others, 1994).

Figure 2. Conceptual controlled area, topographic contours, and sample sites for the upper cliff and caprock samples of the Tiva Canyon Tuff.
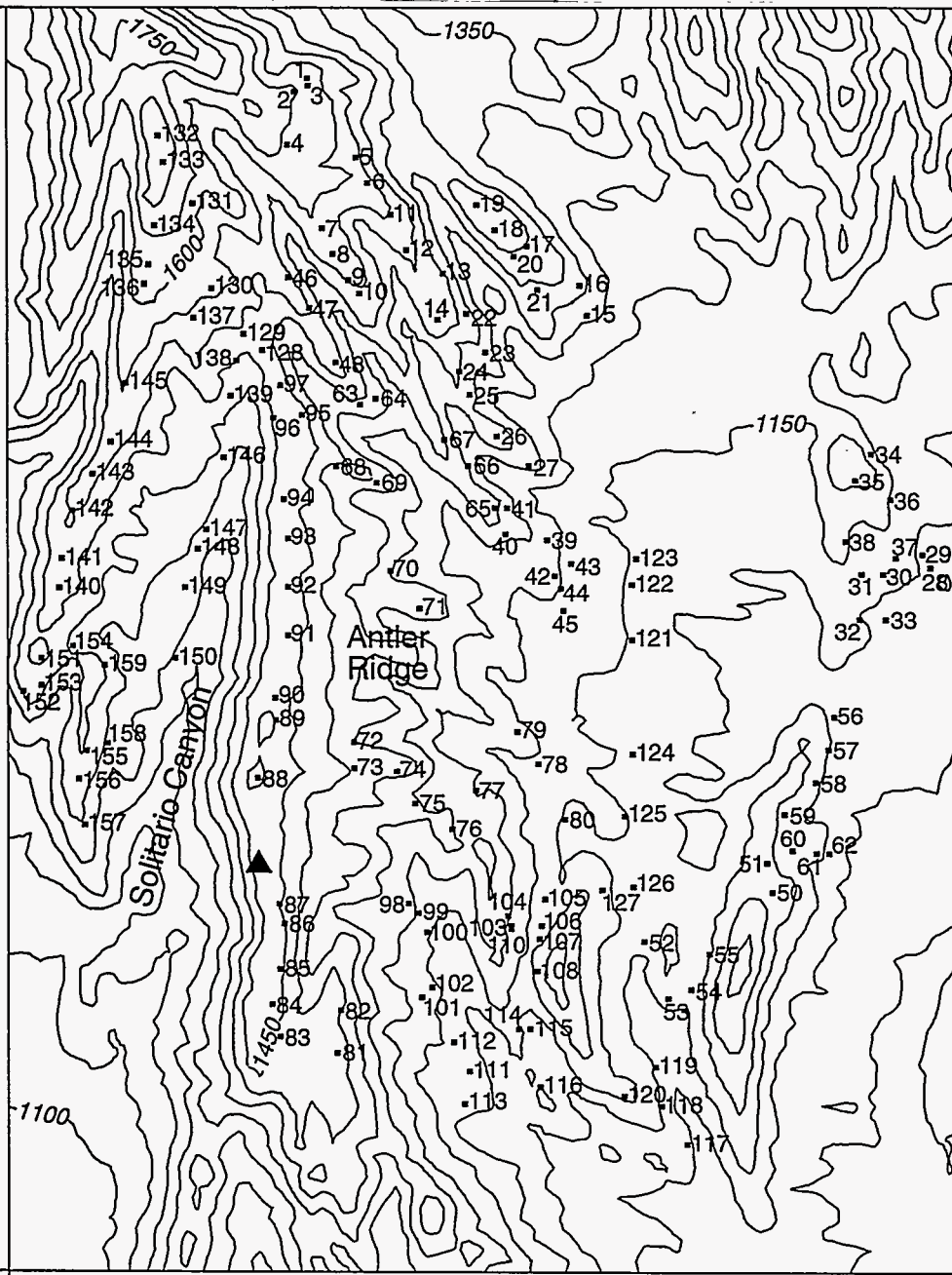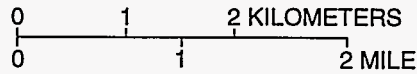
EXPLANATION

∎117   OUTCROP SAMPLE SITE AND NUMBER—See table 3

▲   SOLITARIO CANYON REFERENCE SECTION

—*1450*— TOPOGRAPHIC CONTOUR—Contour interval is 50 meters

The Tiva Canyon Tuff, the uppermost, densely welded tuff of the Miocene Paintbrush Group, is composed of a compositionally zoned, welded ash-flow tuff (Scott and Bonk, 1984). The lower three-fourths of the unit is composed of high-silica rhyolite that is remarkably uniform in composition regardless of the degree of welding or devitrification; the upper one-fourth of the unit is composed of quartz latite that is transitional in composition downward to the high-silica rhyolite (Scott and Bonk, 1984; Flood and others, 1989). The Tiva Canyon Tuff is exposed extensively along ridges and valley walls at Yucca Mountain (Scott and Bonk, 1984). The quartz latite is distinguished from the high-silica rhyolite by the presence of microphenocrysts of biotite, feldspar, and lesser pyroxene, whereas the high-silica rhyolite is generally phenocryst poor (Broxton and others, 1989; Singer and others, 1994).

Approach

Mineralization of volcanic and sedimentary rocks in the Basin and Range Province was a consequence of ascending hydrothermal solutions that, under suitable conditions, deposited minerals of economic interest along and adjacent to the fluid pathways in concentrations sufficient to attract exploration and exploitation. In addition to the deposition of ore minerals, the compositions of the host rocks were affected by the hydrothermal solutions. For example, in carbonate-hosted precious-metal deposits of the Bare Mountain area west of Yucca Mountain, the strontium isotope compositions ($\delta^{87}Sr$) in regions of the host limestones were substantially increased from their primary marine values near zero to positive values in excess of +3 (Peterman and others, 1994). Strontium isotope compositions were modified by radiogenic ^{87}Sr scavenged from older basement rocks that was introduced by hydrothermal solutions.

The isotopic composition of oxygen in the host rocks also is strongly perturbed in these epithermal systems as shown by the extensive studies of mineralized Tertiary igneous rocks of the Western United States (Criss and Taylor, 1986). These and other milestone investigations documenting this phenomenon are summarized in a stable-isotope review volume edited by Valley and others (1986). Terrestrial igneous rocks commonly have primary bulk-rock oxygen isotope compositions ($\delta^{18}O$) in the range of +5.5 to +11.0 ‰ (Taylor and Sheppard, 1986), whereas meteoric waters are strongly depleted in ^{18}O relative to most igneous rocks. For example, ground water in the southern Nevada area has $\delta^{18}O$ values generally between -14 and -13 ‰ (Benson and McKinley, 1985); $\delta^{18}O$ values were probably more negative during past wetter climate periods (Winograd and others, 1988). Where hydrothermal solutions interact with volcanic rocks, oxygen is exchanged between the waters and rocks such that the rock becomes relatively depleted in ^{18}O (lower $\delta^{18}O$ values) and the water becomes enriched in ^{18}O (higher $\delta^{18}O$ values). If the water and rock were to completely equilibrate, their respective $\delta^{18}O$ values would be a function of the temperature-dependent mineral-water fractionation factors and the ratio of the mass of rock to the mass of water; relatively high water/rock ratios, such as those that characterize most hydrothermal systems, can reduce the $\delta^{18}O$ value of the rocks by several permil (Criss and Taylor, 1986). Estimating the actual water/rock ratios of such a system depends on a number of additional factors including the nature of the porosity and permeability of the rock and whether the system is open or closed (Ohmoto, 1986). This phenomenon has been well documented in hydrothermal systems of the Western United States (Criss and Taylor, 1986) where the spatial variability of whole-rock $\delta^{18}O$ values clearly delineates the locus of hydrothermal activity by concentric zones of ^{18}O depletion. Thus, oxygen isotope compositions of Tertiary volcanic rocks can be used at Yucca Mountain to determine whether or not these rocks have interacted with hydrothermal fluids in the past. At low water/rock ratios, the isotopic effect of such interaction likely will be more easily detected than physical manifestations such as mineralogical alteration. This approach was suggested by Taylor (1974), is cited in the geochemical exploration literature (Levinson, 1980), and has been used in northeastern Australia to assess the potential of terrestrial Paleozoic volcanogenic rocks for economic mineral deposits (Ewers and others, 1994).

In addition to the evaluation of potential mineralization by using oxygen isotopes as described above, samples were also analyzed for precious metals (gold and silver) that could have been introduced by hydrothermal fluids and other pathfinder elements such as antimony, arsenic, and mercury, commonly associated with this type of mineralization (Romberger, 1988).

Samples

One-hundred and fifty-seven samples of the upper cliff and caprock zones of the Tiva Canyon Tuff were collected from the conceptual controlled area (fig. 2). Sampling sites were located by superimposing a rectilinear grid with a spacing of 500 m on the geologic map of Yucca Mountain (Scott and Bonk, 1984), and specific sites were selected as close to the grid nodes as possible within the constraints of outcrops of the upper cliff. Map coordinates for samples were obtained using a portable Global Positioning System (GPS) receiver and are accurate to ±100 m. Additionally, 38 samples from a measured stratigraphic section (Geslin and Moyer, U.S. Geological Survey, written commun., 1993) of the Tiva Canyon Tuff at Solitario Canyon were collected. These samples were processed identically to the upper cliff and caprock zone samples; however, only a limited set of geochemical data were obtained from them.

Approximately 1 to 2 kg of sample were collected from outcrops using standard steel hammers. Veins and coatings of surficial calcite, large pumice clasts, and lithic clasts were avoided in collecting the samples. In the laboratory, subsamples were obtained from hand-specimen-size pieces using a 0.5-inch-diameter diamond drill with deionized coolant water. Two cores approximately 2 inches long were taken with emphasis on the rock matrix. The cores were rinsed in deionized water, dried, and pulverized to approximately 200 mesh using a hardened steel ring and puck mill. Splits of the 200-mesh powders were used for oxygen isotope, neutron activation, and x-ray fluorescence analyses.

Methods

Oxygen isotope compositions were measured at the Department of Geological Sciences, University of Saskatchewan, Canada. Oxygen was obtained by decomposition of about 10 mg of a sample powder using bromine pentafluoride. Samples with calcite were leached with 5 percent acetic acid or 10 percent hydrochloric acid prior to analysis. The isotopic composition of oxygen is reported in units of permil deviations ($\delta^{18}O$ values) from Standard Mean Ocean Water (SMOW). Replicate analyses of samples and standards indicate that $\delta^{18}O$ values are reproducible within 0.5 permil. Instrumental neutron activation analysis

was performed by Activation Laboratories, Ltd. in Ontario, Canada. Major elements and common trace elements are determined with a precision of 10 percent or better; uncommon trace elements may have precisions approaching 100 percent at their detection limits. X-ray fluorescence analysis was performed at the U.S. Geological Survey using an energy-dispersive detector; these concentrations are precise to ±10 percent. Accuracy of all geochemical data was assured by calibration to a suite of internationally accepted standards.

Acknowledgments

OXYGEN ISOTOPES AND TRACE ELEMENTS IN THE TIVA CANYON TUFF

The Tiva Canyon Tuff is the uppermost welded unit of the Paintbrush Group and consists of a basal high-silica rhyolite and an overlying unit of quartz latite that were deposited from an eruption of the Timber Mountain-Oasis Valley caldera complex (Lipman and others, 1966) at 12.7 Ma (Sawyer and others, 1994). Where exposed in incised canyons around Yucca Mountain, the crystal-poor high-silica rhyolite is about 100 m thick, and the overlying crystal-rich quartz latite has a thickness of about 30 m. Both units show varying degrees of welding, vesicularity, devitrification, and lithophysal development that have been used by Singer and others (1994) as a basis for dividing the Tiva Canyon Tuff exposed at Antler Ridge into five zones. Although these zones are also present in the section of the Tiva Canyon Tuff exposed at Solitario Canyon, which is part of the present study, there are some subtle distinctions pertinent to the variations in $\delta^{18}O$ values and some elemental contents of the samples.

SOLITARIO CANYON REFERENCE SECTION

Petrography and Geology

Samples collected from a measured reference section of the Tiva Canyon Tuff on the east side of Solitario Canyon (Geslin and Moyer, U.S. Geological Survey, written commun., 1993) traverse a series of zones having distinct physical and petrographic characteristics (table 1, fig. 3). The bottom 13.6 m is a moderately welded tuff consisting predominately of glass shards and 1 to 3 percent phenocrysts of quartz and sanidine. The glass shards are yellow-brown in transmitted light, although a few of the larger fragments have darker cores that may be relict glass less affected by later alteration. Alteration of the shards must be limited to hydration of the glass because alteration minerals are not observed with the petrographic microscope (400 ×). Only samples from this subzone in the Solitario Canyon section contain significant quantities of glass. Spherulitic and axiolitic intergrowths characteristic of devitrification are rare in this subzone, as are lithophysal cavities. This subzone is below the hackly zone of the Antler Ridge section described by Singer and others (1994).

Above the moderately welded subzone of the Solitario Canyon section is 5.1 m of crystal-poor vitric tuff, which is also below the hackly zone in the Antler Ridge section of Singer and others (1994). The degree of devitrification is high at the base of the zone and increases upsection, culminating in complete devitrification at the contact with the overlying lower nonlithophysal zone (table 1). Both devitrification and the presence of lithophysae will have significant effects on the $\delta^{18}O$ values of the whole-rock samples, as will be discussed. The lower nonlithophysal zone, the upper part of which is correlative to the hackly zone at the Antler Ridge section, is a 36 m thick, devitrified welded tuff with shards that are completely microcrystalline to axiolitic. The degree of welding and contents of spherulites and lithophysae increase upsection in this zone grading into the lower lithophysal zone (table 1), a 6.4-m-thick lithology with relatively abundant lithophysae, tridymite-filled microvesicles and granophyric textures. These textures are indicative of relatively slow cooling in this part of the section and crystallization of tridymite and feldspar from a vapor phase (Smith, 1960; Ross and Smith, 1961; Singer and others, 1994).

The next overlying unit exposed at Solitario Canyon is a crystal-poor nonlithophysal zone (30.6 m thick) that corresponds to the clinkstone zone at Antler Ridge (Singer and others, 1994). The Tiva Canyon Tuff in this zone is moderately to densely welded, and the edges of the shards are obscured by microcrystallization or microgranophyres. The tuffs are totally devitrified, as they are in most of the other sections, but fibrous devitrification textures are sparse.

The crystal-poor nonlithophysal zone is overlain by the crystal-rich lithophysal zone near the top of the Solitario Canyon section (table 1, fig. 3). This zone is 13.5 m in thickness and is similar to the lower lithophysal zone, but with more variable, although fewer, lithophysae and pumice fragments. Many of the pumice fragments have granophyric textures, and the moderately welded tuff has been completely devitrified. The abundance of phenocrysts increases upward near the top of the section as this unit grades into the quartz latite in the caprock zone. The lower part of this zone (crystal transition subzone) of the Solitario Canyon section is equivalent to the upper cliff zone described by Singer and others (1994) at Antler Ridge.

Oxygen Isotope and Chemical Compositions

Delta ^{18}O values of whole-rock samples of the Tiva Canyon Tuff from the Solitario Canyon section range from +7.9 to +11.8 ‰ (table 2, fig. 3). This range is within the range reported for pristine siliceous volcanic rocks (Taylor, 1968), unlike the low values (less than 6 ‰) from rhyolites that have been hydrothermally altered or have a genesis involving meteoric waters, brines, or hydrothermally altered crustal rocks (Hildreth and others, 1984; Taylor, 1986). The $\delta^{18}O$ values of the tuffs do not vary systematically with stratigraphic height (fig. 3), although the lowest values are in nonlithophysal zones and the highest values are from the high-silica rhyolite of the lowest unit, the moderately welded subzone with relict glass. Within other zones of the high-silica rhyolite, the $\delta^{18}O$ values are lower than in the glass-rich, moderately welded subzone, but samples with more lithophysae or axiolitic textures tend to have higher values. In the uppermost zones, most values are near +8 ‰, although the highest $\delta^{18}O$ values are in samples having more pumice fragments with microcrystalline or granophyric intergrowths.

Table 1. Lithology and nomenclature of the Tiva Canyon Tuff in the vicinity of Yucca Mountain

[From Buesch and others, 1996]

Map unit	Symbol	Subzone units			Symbols		
Caprock zone	ccr	Crystal-rich	Vitric zone	Nonwelded zone	Tpcr	Tpcrv	Tpcrv3
				Moderately to densely welded subzone			Tpcrv2
				Vitrophyre subzone			Tpcrv1
			Nonlithophysal zone or lithophysal zone	Pumice-rich subzone		Tpcm or Tpcrl	Tpcm (1)4
				Pumice-poor subzone			Tpcm (1)3
				Pumice-rich subzone			Tpcm (1)2
				Transition subzone			Tpcm (1)1
Upper cliff zone	cuc						
Upper lithophysal zone	cul	Crystal-poor	Upper lithophysal zone		Tpcp	Tpcpul	
Clinkstone zone	cks		Middle nonlithophysal zone			Tpcpmn	
Lower lithophysal zone	cll		Lower lithophysal zone			Tpcpll	
Hackly zone	ch		Lower nonlithophysal zone	Hackly subzone		Tpcpln	Tpcplnh
Columnar zone	cc			Columnar subzone			Tpcplnc
			Crystal-poor vitric zone	Vitrophyre subzone		Tpcpv	Tpcpv3
				Moderately to densely welded subzone			Tpcpv2
				Nonwelded to partially welded subzone			Tpcpv1
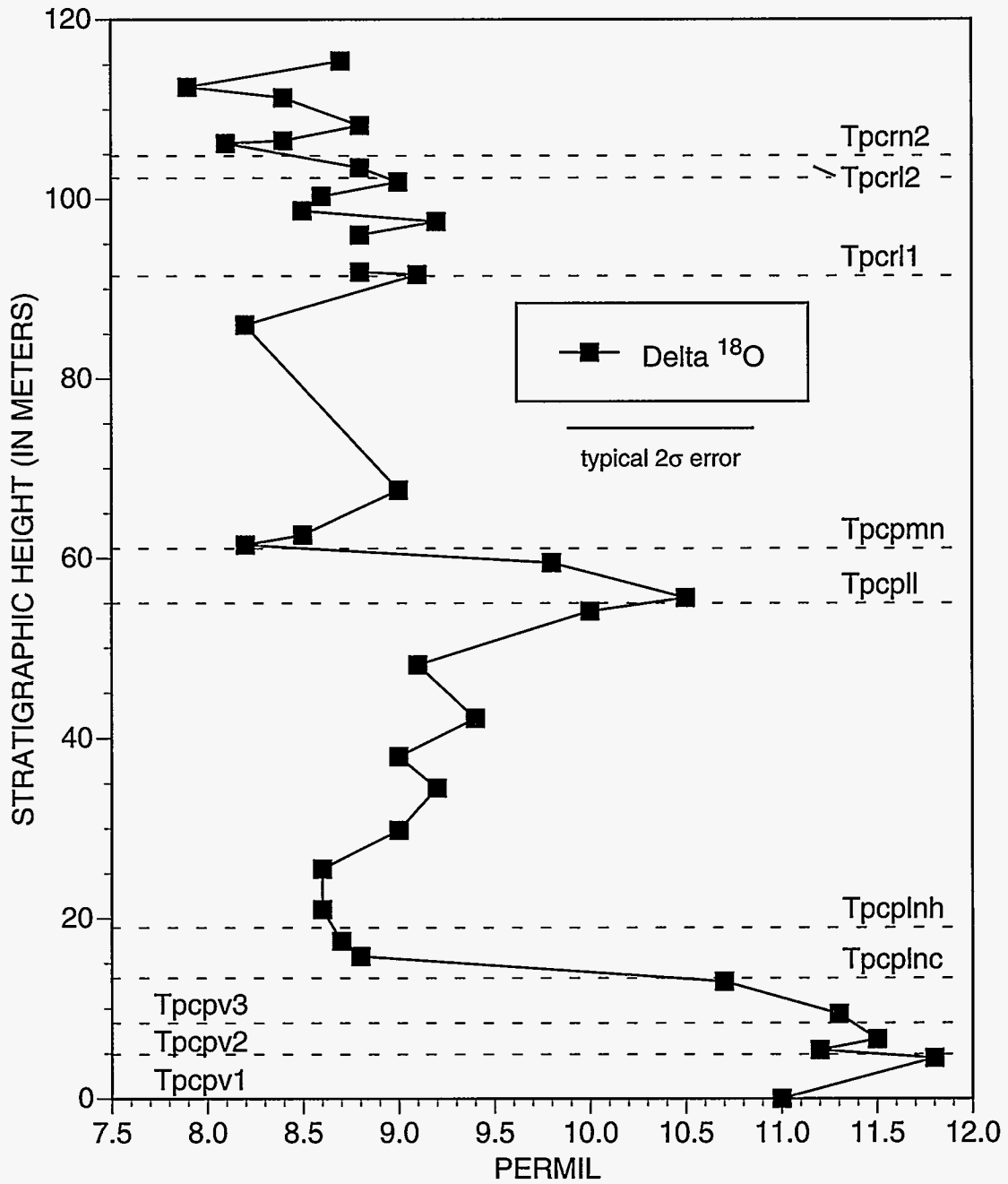
Figure 3. Delta ^{18}O values of whole-rock samples as a function of stratigraphic height in the Tiva Canyon Tuff from the Solitario Canyon reference section. Datum is the base of the Tiva Canyon Tuff. The subunit abbreviations are described in table 1.

Table 2. Geochemistry of the Solitario Canyon reference section at Yucca Mountain

[%, percent; x-ray fluorescence, in ppm by weight except where noted; position indicates stratigraphic distance above base of Tiva Canyon Tuff in meters]

Sample number	Position	K (%)	Ca (%)	Ti	Rb	Sr	Y	Zr	Nb	Ba	La	Ce	$\delta^{18}O$ (‰)
3737	115.4	4.57	0.99	2,328	116	96	42	604	19	867	194	289	8.7
3736	112.5	4.36	1.27	2,116	120	84	42	507	18	679	184	281	7.9
3735	111.3	4.25	0.48	1,760	131	64	42	460	21	565	166	251	8.4
3734	108.2	4.23	0.63	1,906	140	65	45	486	20	500	145	230	8.8
3733	106.5	4.09	1.03	1,552	154	76	41	392	22	366	126	196	8.4
3732	106.2	3.93	1.67	1,326	152	50	37	323	26	270	105	154	8.1
3731	103.5	4.04	2.10	1,394	151	71	41	329	25	294	94	147	8.8
3730	101.9	4.01	0.81	1,484	156	48	40	355	25	271	97	164	9.0
3729	100.3	3.93	1.54	1,409	159	54	39	336	26	225	97	142	8.6
3728	98.7	3.77	0.86	1,322	164	48	44	294	26	191	69	118	8.5
3727	97.5	3.66	0.43	1,118	172	42	40	271	31	167	47	81	9.2
3726	96.0	3.59	0.60	1,065	169	45	42	256	30	158	53	90	8.8
4748	94.0	3.58	0.26	962	180	23	42	226	31	106	53	85	
4747	93.3	3.53	0.51	923	183	23	41	210	30	96	57	82	
3725	91.9	3.58	0.39	840	193	16	41	201	33	67	39	70	8.8
3724	91.6	3.50	0.67	832	183	24	37	195	32	73	59	80	9.1
3723	86.0	3.58	0.48	894	194	23	43	209	32	57	54	68	8.2
3721	67.6	3.51	0.45	865	182	18	38	200	29	65	48	73	9.0
3720	62.6	3.52	0.35	866	189	14	40	201	33	64	49	85	8.5
3719	61.5	3.53	0.45	890	188	24	39	203	32	91	43	71	8.2
3718	59.5	3.53	0.33	873	195	15	41	202	32	70	44	68	9.8
3717	55.6	3.54	0.37	851	187	17	35	197	31	61	44	72	10.5
3716	54.1	3.57	0.86	857	186	20	39	195	32	72	45	74	10.0
3715	48.1	3.61	0.60	891	182	25	38	195	29	84	45	81	9.1
3714	42.2	3.60	0.49	858	189	18	38	200	32	62	57	82	9.4
3713	38.0	3.60	0.28	901	194	13	37	217	35	73	50	79	9.0
3712	34.5	3.53	0.65	869	184	17	41	197	31	58	49	86	9.2
3711	29.8	3.52	0.19	905	185	13	40	209	32	60	43	79	9.0
3710	25.5	3.56	0.37	856	180	14	41	195	32	52	47	74	8.6
3709	21.0	3.50	0.34	882	182	14	39	202	31	64	46	82	8.6
3708	17.5	3.56	0.30	875	184	14	39	202	33	73	54	80	8.7
3707	15.8	3.53	0.28	891	186	11	40	202	30	53	56	85	8.8
3706	13.0	4.09	0.27	833	186	12	39	201	31	40	39	78	10.7
3705	9.4	4.12	0.30	828	181	15	40	203	31	55	51	80	11.3
3704	6.6	3.76	0.35	854	174	21	38	198	31	51	46	64	11.5
3703	5.4	3.39	0.38	867	173	26	39	207	31	50	41	72	11.2
3702	4.5	3.24	0.79	925	157	52	41	211	32	70	43	67	11.8
3701	0.0	3.38	1.26	882	147	82	39	204	33	67	49	73	11.0

In marked contrast to the irregular variation in $\delta^{18}O$ values with stratigraphic height in samples from the Solitario Canyon section, the titanium, zirconium, barium, niobium, lanthanum and cerium contents of the tuffs vary more regularly (table 2, figs. 4–6). The concentrations of most of these elements are lowest and constant in the crystal-poor, high-silica rhyolite, but higher and increase regularly upsection in the crystal-rich zones culminating in quartz latite. Niobium contents in the high-silica rhyolite are slightly higher than in the overlying quartz latite. Inasmuch as the high-silica rhyolite was erupted prior to the quartz latite and presumably represents the top of the magma chamber, the increase in both phenocryst content and concentration of these elements in the quartz latite represents a deeper part of the magma chamber. Virtually identical variations in these elements with stratigraphic position have been reported for other sections of the Tiva Canyon Tuff (Broxton and others, 1989; Peterman and Futa, 1996), the underlying Topopah Spring Tuff (Schuraytz and others, 1989; Flood and others, 1989; Neymark and others, 1995), as well as many Quaternary ash-flow tuffs from other areas, including the Bishop Tuff in California (Hildreth, 1979; 1981) and Los Humeros volcanic center in Mexico (Ferriz and Mahood, 1987). Among the processes that have been proposed to account for these gradients in the chemical composition of silicic magmas are crystal fractionation (Hildreth and Michael, 1983), contamination by roof rocks (Taylor, 1986), selective diffusion (Hildreth, 1979), or combinations of these. Exactly which processes were operating in the magma chamber that produced the apparent gradients in the Tiva Canyon Tuff are as yet unknown and beyond the scope of this study, except to note that the gradients were magmatic in origin and not the result of later alteration.

Concentrations of rubidium, strontium, potassium, and especially calcium in the tuffs from the Solitario Canyon section, vary less regularly with stratigraphic height than most other elements (table 2, figs. 7 and 8). The most significant variation is in the calcium contents of samples from the top of the section. The concentrations of strontium and potassium are higher and the rubidium contents lower in the quartz latite relative to the earlier deposited high-silica rhyolite, but the variation in the contents of these elements within each rock type is greater than that of most other elements. As with most elements, the higher strontium and potassium and lower rubid-

ium contents of the quartz latite, which represents a deeper portion of the magma chamber than the high-silica rhyolite, are typical of the chemical gradients observed in many silicic magma chambers (Hildreth, 1981).

Discussion of Results

Elements such as titanium and zirconium are typically immobile during later alteration events in volcanic rocks (Pearce and Cann, 1973) and, therefore, ratios of their concentrations should reflect magmatic processes. The contents of barium, cerium, zirconium, and niobium not only vary regularly with stratigraphic height, as shown in figures 4–6, but also vary directly with titanium concentrations, and hence with each other, for all lithologies of the Tiva Canyon Tuff from the Solitario Canyon section (fig. 9). The high-silica rhyolite was the first eruption in the series, representing the top of the magma chamber, and is crystal-poor (less than 2 percent phenocrysts) in part because of the paucity of cumulates. In contrast, the quartz latite presumably represents a higher temperature and deeper portion of the chamber that contained significantly more cumulates as evidenced by 5 to 10 percent modal phenocrysts. Thus, the quartz-latite from the top of the Solitario Canyon section is higher in titanium and other compatible elements than the high-silica rhyolite from the lower portions of the section.

Neither the calcium contents nor $\delta^{18}O$ values of samples from the Solitario Canyon section vary regularly with titanium contents (fig. 10). To a lesser extent, the strontium, rubidium, and potassium contents do not vary regularly with titanium contents, especially for samples in which the strontium and potassium contents are the lowest (fig. 9). Given that the elements that correlate directly with titanium contents do so because of magmatic processes, those that do not vary with titanium contents most likely reflect nonmagmatic processes, such as post-eruptive alteration.

The lack of correlation between calcium contents and stratigraphic height can be attributed primarily to capricious amounts of secondary carbonate present in the samples from the Solitario Canyon section. Strontium is less affected because strontium to calcium ratios are higher in the tuff than in pedogenic carbonate. This carbonate has high $\delta^{18}O$ values near +19, similar to those of vein-filling calcite from the
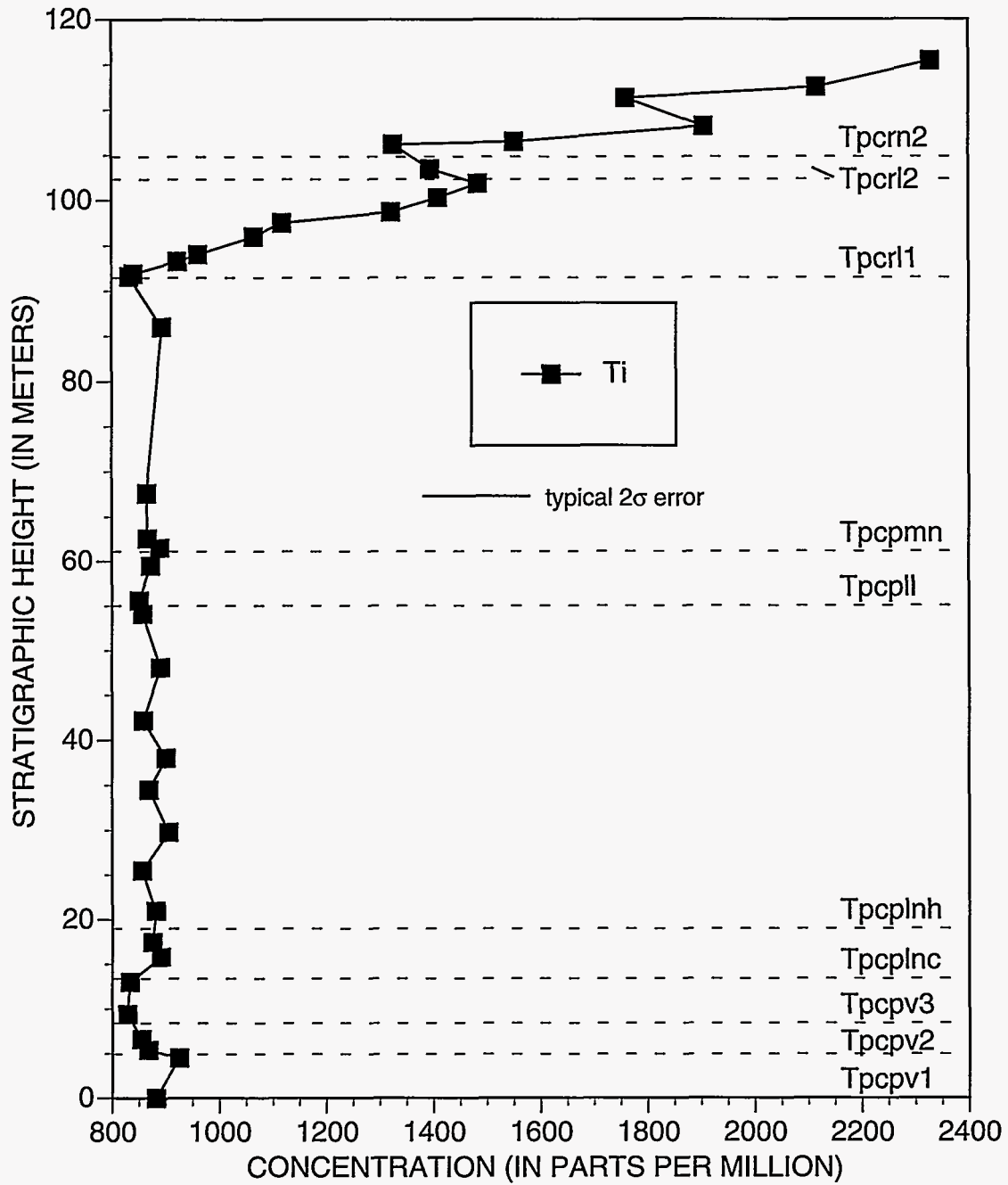
Figure 4. Titanium concentration as a function of stratigraphic height in the Tiva Canyon Tuff from the Solitario Canyon reference section. Datum and abbreviations as in figure 3.
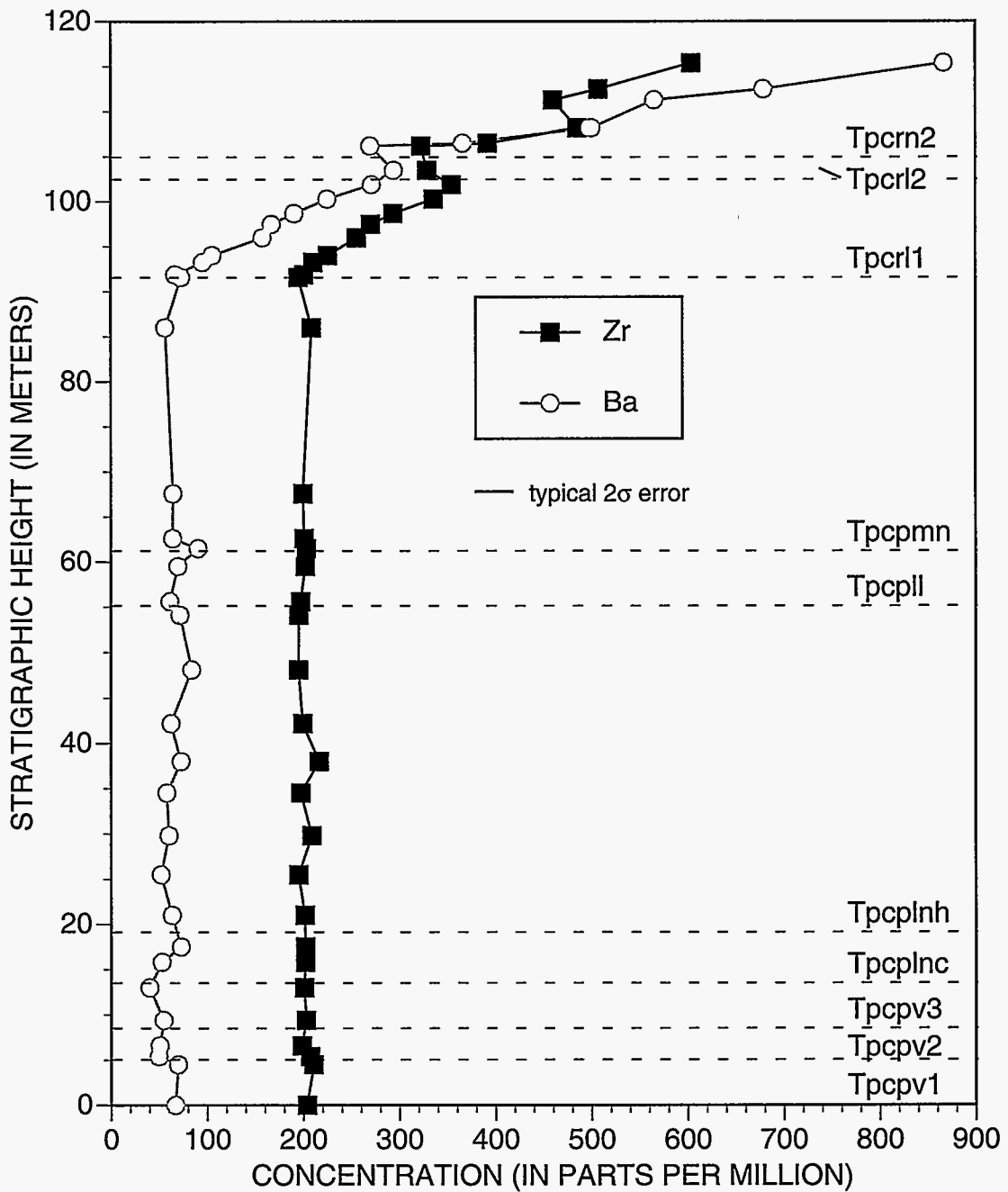
Figure 5. Zirconium and barium concentrations as a function of stratigraphic height in the Tiva Canyon Tuff from the Solitario Canyon reference section. Datum and abbreviations as in figure 3.
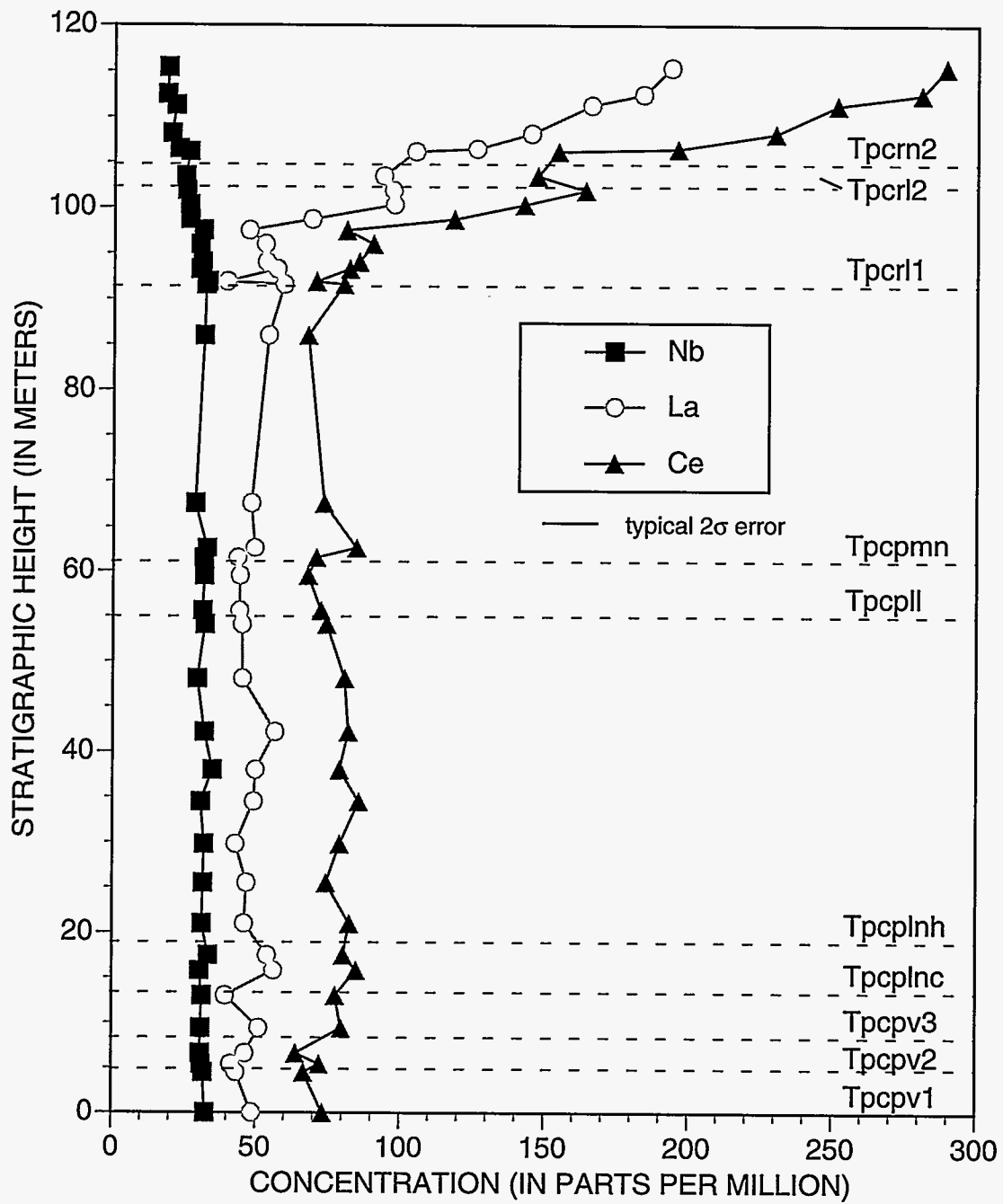
Figure 6. Niobium, lanthanum, and cerium concentrations as a function of stratigraphic height in the Tiva Canyon Tuff from the Solitario Canyon reference section. Datum and abbreviations as in figure 3.
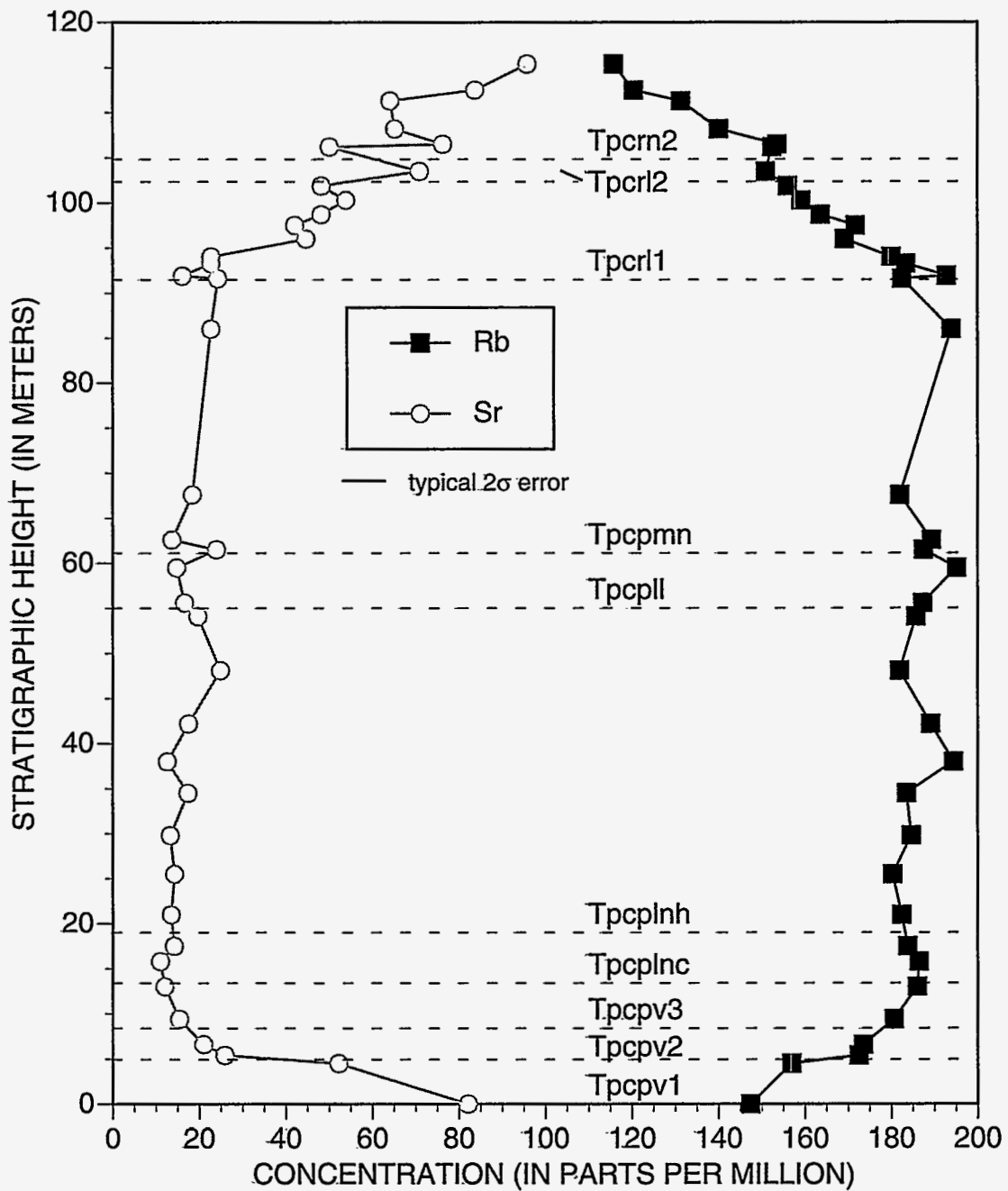
Figure 7. Rubidium and strontium concentrations as a function of stratigraphic height in the Tiva Canyon Tuff from the Solitario Canyon reference section. Note the variations in concentration near the base of the section. Datum and abbreviations as in figure 3.
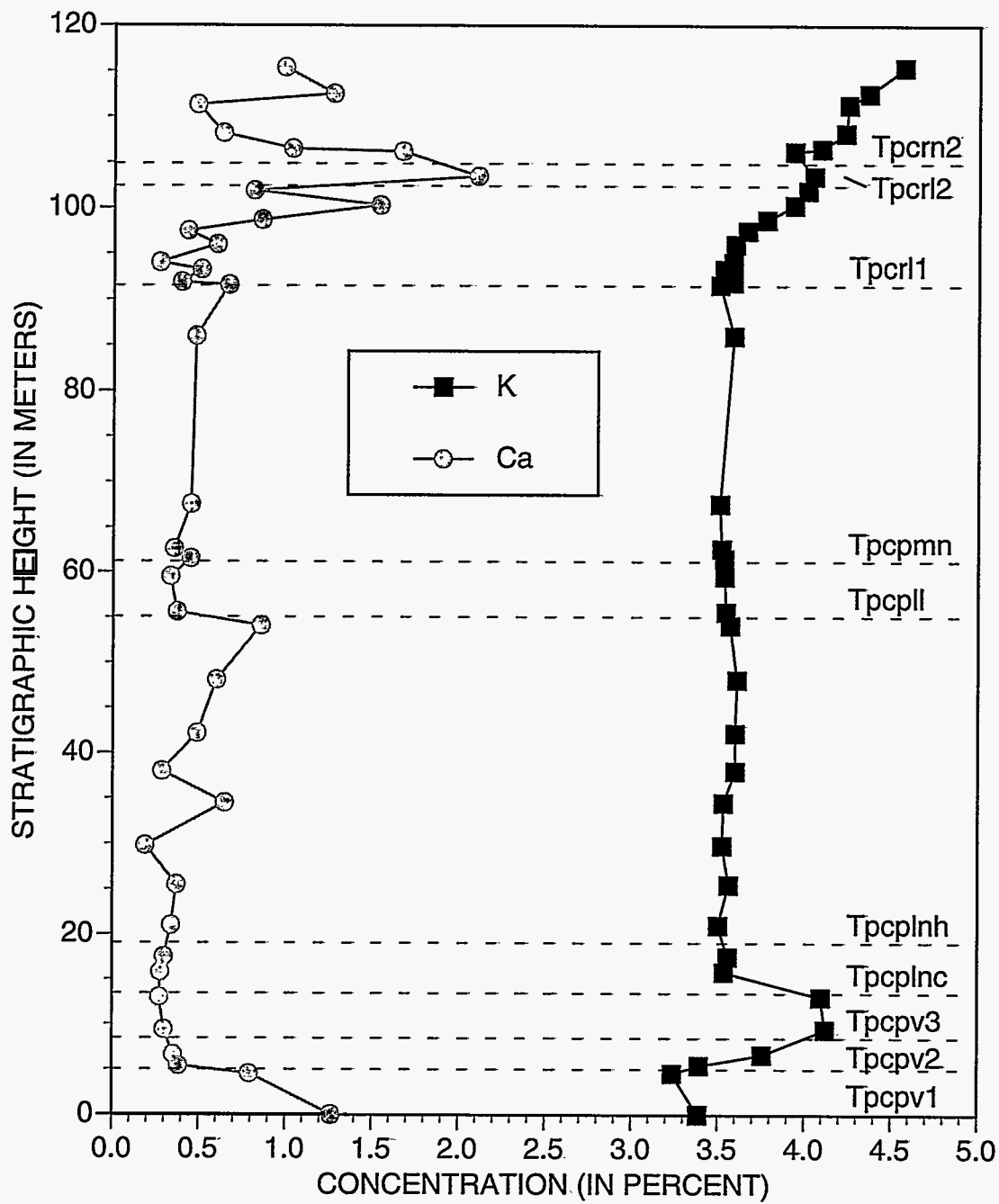
Figure 8. Potassium and calcium concentrations as a function of stratigraphic height in the Tiva Canyon Tuff from the Solitario Canyon reference section. Note the general scatter in calcium and the variations in both elements near the base of the unit. Datum and abbreviations as in figure 3; typical 2σ errors are within the size of the symbols.
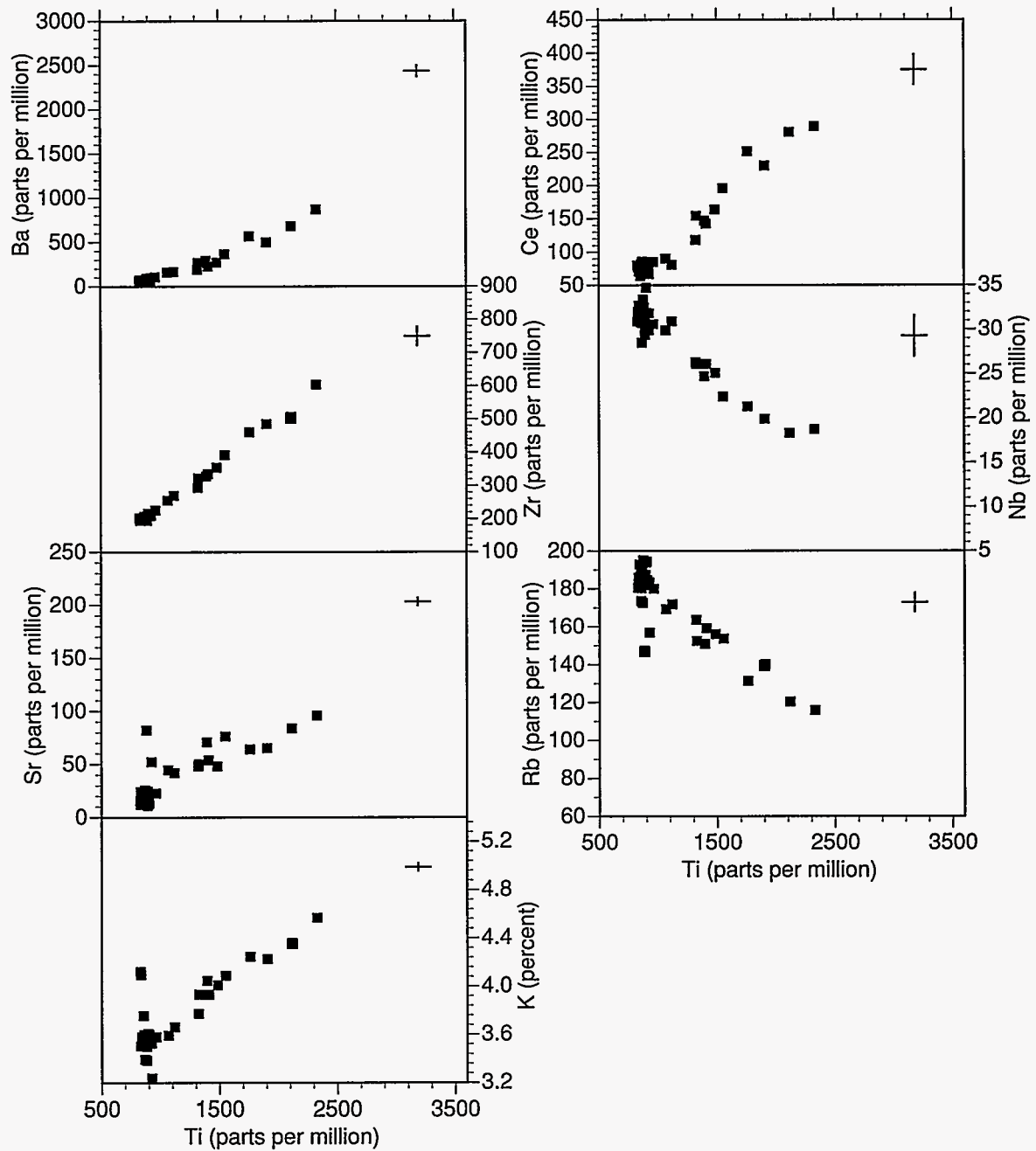
Figure 9. Variations of barium, cerium, zirconium, niobium, strontium, rubidium, and potassium concentrations as a function of titanium concentration in the Solitario Canyon reference section. The trends in these elements are typical of differentiation in magmatic systems. Note the greater scatter in rubidium, strontium, and potassium at low titanium concentrations. Typical 2σ errors are shown by the crosses.
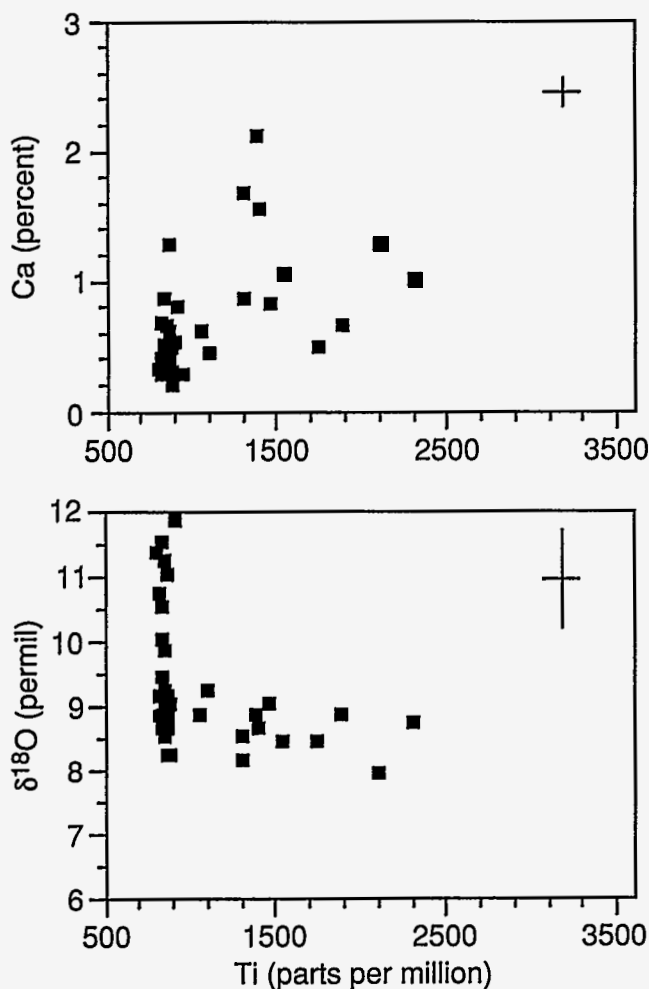
Figure 10. Variation of calcium and $\delta^{18}O$ as a function of titanium concentration in the Solitario Canyon reference section. Enrichments in ^{18}O relative to the estimated original magmatic values of +6 to +8 ‰ are evident as well as significant variation in calcium contents; these trends are atypical of pristine igneous rocks. Typical 2σ errors are shown by the crosses.

Yucca Mountain area and was formed via precipitation from meteoric waters at temperatures of about 25°C (Szabo and Kyser, 1990). Whole-rock $\delta^{18}O$ values should not be affected by this process because the maximum amount of secondary carbonate (as estimated from both petrographic observations and the amounts of added calcium) is less than 5 percent, thereby resulting in a maximum increase of about 0.5 ‰. Furthermore, samples were selected to minimize the amount of secondary carbonate, and many samples were treated with acetic or hydrochloric acid to remove any small amount of carbonate present. The only other elements that would be affected by

low-temperature fluids would be those that are easily mobilized by meteoric waters, such as rubidium, potassium, and strontium. The lack of correlations between potassium and titanium and between strontium and titanium is most pronounced in samples with the lowest potassium and strontium contents (fig. 9), as would be expected if these elements were affected by low-temperature fluids. On the other hand, rubidium contents are most variable in samples with the highest rubidium concentrations, which may simply indicate samples most affected by alteration because rubidium is so easily mobilized relative to most other elements. The effect of this low-temperature alteration was both subtle and differential in that those components most likely to have been affected, namely $\delta^{18}O$ values, calcium, rubidium, potassium, and strontium, do not correlate with each other.

The original $\delta^{18}O$ values of high-silica rhyolite and quartz latite prior to any post-eruptive alteration can be ascertained from the isotopic composition of phenocrysts and the values reported for other ash-flow tuffs. Lipman and Friedman (1975) and Farmer and others (1991) reported $\delta^{18}O$ values of +6.4 to +7.0 for sanidine phenocrysts in samples of the Tiva Canyon Tuff, and +6.8 to +8.1 for sanidine phenocrysts from the underlying Topopah Spring Tuff. These data imply magmatic $\delta^{18}O$ values of about +7 to +8 ‰ because the fractionation of oxygen isotopes between felsic silicate liquids and feldspar is small (Taylor and Epstein, 1962). Although the oxygen isotopic composition of the Tiva Canyon Tuff magma may have varied because of the irregular distribution of phenocrysts or interaction between the top of the magma and country rocks, other studies of genetically related ash-flow tuffs (Halliday and others, 1984; Taylor, 1991) indicate that such variations are usually less than 1 ‰, thereby constraining the original $\delta^{18}O$ values of the high-silica rhyolite and quartz latite of the Solitario Canyon section to between +6 and +8 ‰. In addition, Halliday and others (1984) reported $\delta^{18}O$ values from +6.7 to +8.0 for sanidine phenocrysts from the Bishop Tuff, and McCulloch and others (1994) measured $\delta^{18}O$ values from +6.1 to +7.0 for feldspar phenocrysts in rhyolites from the Taupo volcanic zone of New Zealand. A range of +6.3 to +7.3 for the $\delta^{18}O$ values has been reported for feldspars in rhyolites from the Los Humeros volcanic center in Mexico (Ferriz and Mahood, 1987), and Taylor (1991) suggests values of +6 to +8 for the historic Obsidian Dome rhyolites from

the Inyo volcanic chain in California. Only the Yellowstone rhyolites, for which $\delta^{18}O$ values of quartz phenocrysts range from +0.7 to +7.7 (Hildreth and others, 1984), have significant variations in their phenocryst and whole-rock values. Such low $\delta^{18}O$ values have been attributed to contributions from meteoric waters (Hildreth and others, 1984) or from hydrothermally altered country rocks (Taylor, 1986) added to the magma prior to eruption, processes that are clearly not recorded by the $\delta^{18}O$ values of the tuffs from the Solitario Canyon section.

Only a few of the samples from the Solitario Canyon section have whole-rock $\delta^{18}O$ values near those estimated for the original magma, and most are higher. In the few studies that report both phenocryst and whole-rock $\delta^{18}O$ values of the same sample, the whole-rock values are usually near, but can be significantly higher or lower than, the original magmatic values estimated from the phenocrysts. For example, Stuckless and O'Neil (1973) reported significantly higher $\delta^{18}O$ values (up to +20.5 ‰) for whole-rock samples relative to phenocrysts of silicic volcanic rocks from the Superstition-Superior area in Arizona. They proposed that the high values resulted from low-temperature alteration, including hydration of volcanic glass, a process that Taylor (1968) demonstrated could substantially increase the $\delta^{18}O$ value of glass. In another study, three out of the six samples of the Bishop Tuff examined by Halliday and others (1984) have whole-rock $\delta^{18}O$ values that are less than 1 permil higher than those of their sanidine phenocrysts. Whole-rock values in two samples are significantly higher, but lower in another, relative to their sanidine phenocrysts. Elevation of the whole-rock $\delta^{18}O$ values was attributed to low-temperature exchange with ground waters, whereas ^{18}O depletions of the whole rock result from post-emplacement, hydrothermal alteration.

The conspicuous lack of any whole-rock $\delta^{18}O$ values less than those of the original magma in the Solitario Canyon section indicates that these samples have not been affected by hydrothermal alteration. Moreover, the lack of correlation between $\delta^{18}O$ values and titanium contents, the latter of which appear to faithfully record magmatic processes, indicates that variations in the oxygen isotopic composition of samples from the Solitario Canyon section are not magmatic. The $\delta^{18}O$ values of samples from the Solitario Canyon section do not vary with the contents of any of the elements measured, including those elements that

correlate poorly with titanium, such as calcium. However, $\delta^{18}O$ values do correlate with certain petrographic features of the samples.

The highest $\delta^{18}O$ values are in the samples from the base of the section (fig. 3) where the glass contents are highest. These glasses have petrographic characteristics typical of oxidation and hydration. Ross and Smith (1955), Friedman and Smith (1960), Taylor (1968), and Taylor (1991) have demonstrated that hydration of silicic volcanic glass by meteoric waters at low temperatures results in high $\delta^{18}O$ values. This process is analogous to the formation of alteration minerals at low temperatures wherein the alteration product is enriched in ^{18}O by up to 30 ‰ relative to the water. Hydration, and the concomitant increase in $\delta^{18}O$ value of the glass, is ubiquitous in all volcanic glasses because of their inherent instability in low-temperature environments and is absent only in young (less than 1 Ma) volcanic glasses. Hydration of volcanic glass in the basal zone of the Solitario Canyon section via exchange with low-temperature meteoric water with $\delta^{18}O$ values near -12 ‰ (Benson and McKinley, 1985) could easily result in glass with $\delta^{18}O$ values as high as +11.8 ‰.

The lowest $\delta^{18}O$ values are in nonlithophysal zones (fig. 3), although most of these are slightly elevated relative to primary magmatic values. These tuffs are totally devitrified and, therefore, were not altered by hydration but could have exsolved volatiles from the glass as it crystallized during cooling. Those samples with higher granophyric, spherulitic, and vapor-phase mineral components tend to be more ^{18}O rich than proximal samples where these components are less abundant (fig. 3). Thus, intervals of the Tiva Canyon Tuff in this section that were more affected by the fluids exsolving from the slowly cooling ash-flow have slightly more elevated $\delta^{18}O$ values.

Exsolution of fluids and crystallization of the glass shards occur at subsolidus temperatures (less than 600°C), and the fluids released are likely to have $\delta^{18}O$ values equal to, or in excess of, those of the original glass. Quartz and feldspar precipitated at 600°C would be enriched in ^{18}O by 2 and 4 ‰, respectively, relative to the fluid, if the minerals and fluid were in isotopic equilibrium. Thus, recrystallization of slowly cooling tuffs, especially in the presence of deuteric fluids released during devitrification, could result in higher $\delta^{18}O$ values in some samples. In support of this process, $\delta^{18}O$ values of +11.1 and +12.5 have been measured in vapor-phase tridymite from the

underlying Topopah Spring Tuff (Moscati and Whelan, U.S. Geological Survey, written commun., 1995). As with post-emplacement hydrothermal alteration, ground water trapped in the ash-flow and involved with recrystallization of the tuffs would have resulted in lower $\delta^{18}O$ values of the whole-rock samples, instead of the relatively high values observed in this study. Only deuteric alteration would result in slightly elevated $\delta^{18}O$ values relative to estimated original magmatic values.

Taylor (1991) reported only small differences in the $\delta^{18}O$ values of obsidian, vesicular glass, devitrified glass, and pumice from the Obsidian Dome rhyolite in California. However, these rhyolitic tephra and ash-flows, which were emplaced only 600 years ago, have hydrogen isotopic compositions and volatile contents that indicate that the hydrous melts had extensively degassed prior to and during eruption so that devitrification occurred after degassing. These results contrast with those from the tuffs of the Solitario Canyon section, in that the Tiva Canyon Tuff is significantly older, contains glass that has been hydrated, and was most likely degassed as a result of devitrification. Moreover, a few rhyolitic dike rocks from the Obsidian Dome area have slightly lower $\delta^{18}O$ values than most of the other samples because of later hydrothermal alteration. The lack of low $\delta^{18}O$ values from the Solitario Canyon section indicates that hydrothermal alteration has not affected these samples.

UPPER CLIFF AND CAPROCK ZONES

Geology

Samples of the upper cliff and caprock zones of the Tiva Canyon Tuff were collected from throughout the conceptual controlled area (fig. 2). The upper cliff zone was sampled preferentially, but limited exposure dictated that the stratigraphically higher caprock zone was sampled in many cases. Samples from the stratigraphically lower portions of the outcrops are equivalent to the uppermost part of the Solitario Canyon reference section (both upper cliff and caprock zones). Lithologically distinct samples within the caprock zone have higher phenocryst contents and are more reddish; they are less welded and therefore tend to have a higher secondary carbonate content. These samples are also characterized by barium contents in

excess of 1,500 ppm and represent the quartz latite (Flood and others, 1989) within the caprock zone. For the purposes of the following discussion, we refer to these lithologically distinct samples as the caprock zone. These samples are within the upper portion of the caprock zone as defined by Scott and Bonk (1984).

Oxygen Isotope and Chemical Compositions

Delta ^{18}O values for samples from the upper cliff and caprock zones range from +6.9 to +11.8 (table 3), virtually identical to the range of values from the Solitario Canyon section. Most of these $\delta^{18}O$ values are higher than estimated original magmatic values of approximately +6 to +8, and none are less. There is no relation between $\delta^{18}O$ values and proximity to known faults in the area or other geologic features; there is little spatial regularity to the oxygen isotope compositions in general (fig. 11).

The concentrations of barium, cerium, zirconium, niobium, strontium, rubidium, potassium, and thorium vary regularly with titanium contents in the upper cliff and caprock zone samples (tables 4, 5, and 6; fig. 12), overlapping and exceeding the contents of these elements in samples from the Solitario Canyon section. The trends with titanium contents for barium, cerium, and potassium in the caprock zone samples are distinct from those from the upper cliff zone, whereas the other elemental trends in the upper cliff zone samples overlap and are continuous with those from the caprock zone (fig. 12). The higher titanium contents of samples from the caprock zone relative to those from the upper cliff zone reflect a higher phenocryst content and, by inference, a deeper and less siliceous portion of the magma chamber. The trends in these elements are virtually identical to those in samples of the Tiva Canyon Tuff from the Solitario Canyon section and in ash-flow units in general and are emblematic of the magmatic processes that operate in these systems. The rare earth elements also show typical magmatic trends (figs. 12 and 13), with the upper cliff samples showing a relative depletion in europium, probably resulting from crystal fractionation of plagioclase phenocrysts in the high-silica rhyolite.

Calcium, sodium, iron, and uranium contents and $\delta^{18}O$ values for samples of the upper cliff and caprock zones do not correlate as well as other

Table 3. Map coordinates, sample numbers, and oxygen isotope compositions of the Tiva Canyon Tuff

[Sample site number plotted on figure 2; Universal Transverse Mercator coordinates in Zone 11]

Sample site number	Sample number	UTM easting	UTM northing	$\delta^{18}O$ (‰)
1	MR-1000	547841	4083341	10.1
2	MR-1001	547718	4083217	8.6
3	MR-1002	547842	4083279	9.2
4	MR-1003	547647	4082724	8.4
5	MR-1004	548291	4082604	8.5
6	MR-1005	548409	4087905	8.1
7	MR-1006	547973	4081924	8.2
8	MR-1007	548073	4081678	9.1
9	MR-1008	548223	4081433	7.7
10	MR-1009	548323	4081310	7.6
11	MR-1010	548616	4082051	7.4
12	MR-1011	548766	4081713	7.2
13	MR-1012	549114	4081499	8.9
14	MR-1013	549067	4081068	8.8
15	MR-1014	550478	4081107	6.9
16	MR-1015	550402	4081384	8.8
17	MR-1016	549905	4081751	8.6
18	MR-1017	549607	4081903	9.3
19	MR-1018	549432	4082148	8.2
20	MR-1019	549782	4081657	8.2
21	MR-1020	550006	4081351	7.6
22	MR-1021	549339	4081131	8.0
23	MR-1022	549514	4080762	8.7
24	MR-1023	549268	4080576	8.0
25	MR-1024	549368	4080361	8.5
26	MR-1025	549618	4079962	8.4
27	MR-1026	549917	4079686	8.4
28	MR-1027	553712	4078723	8.4
29	MR-1028	553636	4078846	8.1
30	MR-1029	553266	4078659	8.8
31	MR-1030	553068	4078657	9.4
32	MR-1031	553046	4078226	9.2
33	MR-1032	553294	4078227	8.6
34	MR-1033	553160	4079798	8.4
35	MR-1034	553013	4079551	9.2
36	MR-1035	553336	4079368	9.1
37	MR-1036	553389	4078813	9.2
38	MR-1037	552918	4078965	9.2
39	MR-1038	550094	4078978	7.7
40	MR-1039	549698	4079038	8.5
41	MR-1040	549721	4079284	9.2
42	MR-1041	550171	4078640	8.2
43	MR-1042	550319	4078764	8.6
44	MR-1043	550221	4078517	8.7

Table 3. Map coordinates, sample numbers, and oxygen isotope compositions of the Tiva Canyon Tuff—Continued

[Sample site number plotted on figure 2; Universal Transverse Mercator coordinates in Zone 11]

Sample site number	Sample number	UTM easting	UTM northing	$\delta^{18}O$ (‰)
45	MR-1044	550247	4078301	8.5
46	MR-1045	547654	4081460	9.4
47	MR-1046	547853	4081184	8.6
48	MR-1047	548104	4080662	9.4
50	MR-1049	552220	4075632	10.8
51	MR-1050	552169	4075909	10.4
52	MR-1051	551009	4075163	9.7
53	MR-1052	551235	4074609	9.0
54	MR-1053	551457	4074703	10.0
55	MR-1054	551629	4075043	9.3
56	MR-1055	552804	4077300	9.5
57	MR-1056	552756	4076991	11.8
58	MR-1057	552635	4076683	10.3
59	MR-1058	552339	4076373	9.4
60	MR-1059	552416	4076034	8.4
61	MR-1060	552639	4076005	9.8
62	MR-1061	552763	4076005	8.8
63	MR-1062	548329	4080262	9.6
64	MR-1063	548477	4080325	7.1
65	MR-1064	549597	4079284	7.6
66	MR-1065	549347	4079683	7.1
67	MR-1066	549123	4079928	8.3
68	MR-1067	548109	4079676	7.9
69	MR-1068	548482	4079524	8.8
70	MR-1069	548610	4078692	8.8
71	MR-1070	548885	4078324	9.2
72	MR-1071	548273	4077057	9.8
73	MR-1072	548274	4076811	8.4
74	MR-1073	548671	4076782	9.5
75	MR-1074	548846	4076475	8.3
76	MR-1075	549194	4076231	9.4
77	MR-1076	549415	4076602	9.2
78	MR-1077	550008	4076852	10.2
79	MR-1078	549808	4077159	9.5
80	MR-1079	550259	4076329	8.2
81	MR-1200	548116	4074098	9.3
82	MR-1201	548139	4074499	8.9
83	MR-1202	547570	4074249	9.6
84	MR-1203	547494	4074557	9.7
85	MR-1204	547567	4074896	9.5
86	MR-1205	547614	4075328	9.6
87	MR-1206	547563	4075513	10.7
88	MR-1207	547358	4076713	9.2
89	MR-1208	547529	4077269	8.1

Table 3. Map coordinates, sample numbers, and oxygen isotope compositions of the Tiva Canyon Tuff—Continued

[Sample site number plotted on figure 2; Universal Transverse Mercator coordinates in Zone 11]

Sample site number	Sample number	UTM easting	UTM northing	$\delta^{18}O$ (‰)
90	MR-1209	547527	4077485	9.3
91	MR-1210	547648	4078071	8.9
92	MR-1211	547645	4078533	7.5
93	MR-1212	547643	4078995	9.5
94	MR-1213	547616	4079365	7.7
95	MR-1214	547785	4080167	8.1
96	MR-1215	547513	4080135	8.2
97	MR-1216	547585	4080443	8.1
98	MR-1217	548777	4075519	9.3
99	MR-1218	548877	4075428	8.8
100	MR-1219	548952	4075243	9.0
101	MR-1220	548906	4074627	9.7
102	MR-1221	549005	4074720	8.9
103	MR-1222	549745	4075279	9.2
104	MR-1223	549719	4075402	9.7
105	MR-1224	550065	4075558	10.0
106	MR-1225	550042	4075311	10.6
107	MR-1226	550018	4075188	8.8
108	MR-1227	549995	4074879	9.4
110	MR-1229	549744	4075309	10.2
111	MR-1230	549356	4073920	10.9
112	MR-1231	549206	4074197	8.5
113	MR-1232	549308	4073612	8.8
114	MR-1233	549824	4074324	10.6
115	MR-1234	549924	4074324	9.9
116	MR-1235	550026	4073770	8.5
117	MR-1236	551417	4073224	9.8
118	MR-1237	551167	4073592	9.7
119	MR-1238	551115	4073962	8.6
120	MR-1239	550819	4073683	8.3
121	MR-1240	550893	4078028	7.7
122	MR-1241	550889	4078552	8.6
123	MR-1242	550937	4078798	8.3
124	MR-1243	550899	4076949	9.0
125	MR-1244	550828	4076363	10.4
126	MR-1245	550907	4075686	9.3
127	MR-1246	550609	4075653	7.5
128	MR-1300	547410	4080781	9.2
129	MR-1301	547236	4080934	8.7
130	MR-1302	546936	4081364	8.1
131	MR-1303	546759	4082164	7.8
132	MR-1304	546433	4082809	8.7
133	MR-1305	546484	4082563	8.6
134	MR-1306	546389	4081946	8.9

Table 3. Map coordinates, sample numbers, and oxygen isotope compositions of the Tiva Canyon Tuff—Continued

[Sample site number plotted on figure 2; Universal Transverse Mercator coordinates in Zone 11]

Sample site number	Sample number	UTM easting	UTM northing	$\delta^{18}O$ (‰)
135	MR-1307	546341	4081576	8.8
136	MR-1308	546293	4081391	9.0
137	MR-1309	546765	4081086	9.0
138	MR-1310	547163	4080687	7.8
139	MR-1311	547115	4080348	8.7
140	MR-1312	545491	4078521	9.1
141	MR-1313	545514	4078799	9.7
142	MR-1314	545611	4079261	9.5
143	MR-1315	545807	4079601	9.1
144	MR-1316	545979	4079910	8.8
145	MR-1317	546124	4080466	9.0
146	MR-1318	547044	4079762	9.2
147	MR-1319	546875	4079083	9.7
148	MR-1320	546801	4078898	9.2
149	MR-1321	546680	4078528	8.2
150	MR-1322	546584	4077849	7.7
151	MR-1323	545321	4077842	9.8
152	MR-1324	545149	4077533	10.0
153	MR-1325	545322	4077596	8.7
154	MR-1326	545618	4077967	10.4
155	MR-1327	545747	4076982	9.3
156	MR-1328	545674	4076704	9.4
157	MR-1329	545726	4076273	10.3
158	MR-1330	545945	4077044	8.3
159	MR-1331	545916	4077784	7.8
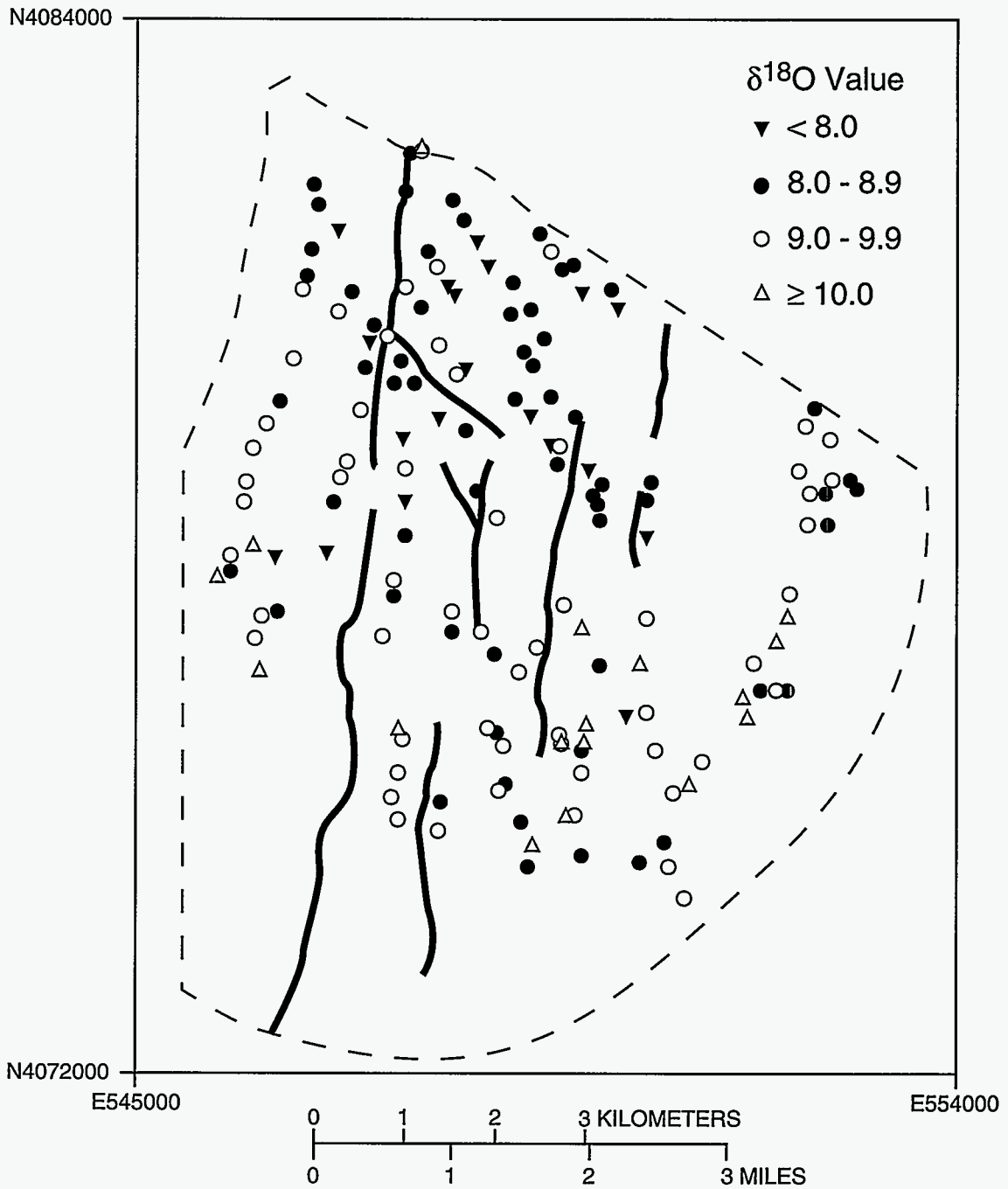
Figure 11. Conceptual controlled area and $\delta^{18}O$ values for the upper cliff and caprock zones. Areas of high $\delta^{18}O$ indicate more post-eruptive low-temperature alteration and lithophysal crystallization of silica. Fault traces generalized from O'Neill and others (1992).

Table 4. Chemistry of major elements

[In percent by weight]

Sample site number	Na[1]	K[2]	Ca[2]	Ti[2]	Fe[1]
1	3.06	4.22	0.53	0.23	1.23
2	3.04	4.31	0.89	0.28	1.33
3	3.06	4.25	1.26	0.24	1.28
4	3.07	4.22	1.09	0.25	1.33
5	3.16	4.29	0.71	0.24	1.26
6	3.01	4.41	0.69	0.26	1.24
7	3.00	4.56	1.15	0.26	1.28
8	2.93	4.35	1.05	0.26	1.22
9	3.08	4.36	0.72	0.26	1.33
10	3.08	4.30	0.87	0.23	1.30
11	3.00	4.48	1.21	0.28	1.29
12	2.88	4.20	0.80	0.26	1.27
13	2.94	4.93	2.17	0.33	1.50
14	3.02	4.32	1.29	0.24	1.21
15	3.15	4.57	1.23	0.21	1.28
16	3.04	4.23	0.79	0.23	1.36
17	2.80	4.18	0.94	0.21	1.15
18	2.93	4.19	0.72	0.23	1.22
19	3.00	4.97	1.57	0.30	1.40
20	3.13	4.31	0.85	0.25	1.28
21	3.22	5.16	0.95	0.32	1.58
22	3.14	4.31	0.92	0.25	1.33
23	3.39	4.75	1.15	0.24	1.44
24	3.38	5.00	1.17	0.30	1.65
25	3.18	4.98	2.57	0.28	1.41
26	3.15	4.85	1.37	0.25	1.34
27	3.36	4.68	0.73	0.23	1.47
28	3.17	4.72	0.63	0.24	1.37
29	3.32	4.84	1.10	0.27	1.55
30	3.19	4.41	0.78	0.20	1.17
31	3.13	4.46	1.77	0.21	1.31
32	3.36	4.72	0.54	0.22	1.40
33	3.48	4.68	1.19	0.24	1.49
34	3.56	4.53	0.57	0.21	1.41
35	3.29	4.69	3.32	0.23	1.45
36	3.54	4.38	0.49	0.19	1.28
37	3.42	4.36	0.72	0.19	1.26
38	3.37	4.58	0.96	0.23	1.45
39	3.28	4.10	0.42	0.17	1.07
40	3.53	4.81	0.63	0.24	1.56
41	3.43	4.60	0.86	0.22	1.45
42	3.66	4.81	0.66	0.25	1.60
43	3.49	4.84	1.19	0.23	1.51
44	3.27	4.51	1.77	0.19	1.24

Table 4. Chemistry of major elements—Continued

[In percent by weight]

Sample site number	Na[1]	K[2]	Ca[2]	Ti[2]	Fe[1]
45	3.33	4.33	0.53	0.19	1.24
46	3.47	4.66	0.69	0.23	1.37
47	3.45	4.35	0.51	0.20	1.32
48	3.82	4.93	0.76	0.30	1.78
50	3.57	4.49	0.50	0.20	1.28
51	3.05	3.71	1.12	0.08	0.70
52	3.35	4.52	0.91	0.21	1.34
53	3.27	4.56	1.33	0.21	1.34
54	2.96	3.72	1.99	0.09	0.74
55	3.24	4.63	2.47	0.22	1.27
56	3.43	3.99	0.49	0.15	1.16
57	3.34	4.28	0.90	0.18	1.27
58	3.58	4.31	0.46	0.18	1.25
59	3.70	4.60	0.58	0.21	1.42
60	3.64	4.80	0.56	0.23	1.41
61	3.44	4.41	0.57	0.20	1.34
62	3.46	4.24	0.41	0.18	1.22
63	3.25	3.82	0.35	0.12	0.99
64	3.66	4.65	0.56	0.22	1.55
65	3.47	4.63	1.62	0.22	1.36
66	3.70	4.76	0.69	0.25	1.52
67	3.41	4.65	0.60	0.22	1.43
68	3.16	4.65	0.80	0.24	1.36
69	3.36	4.36	0.54	0.20	1.23
70	3.33	4.29	0.48	0.17	1.16
71	3.26	4.06	0.86	0.16	1.07
72	3.22	3.58	0.24	0.09	0.77
73	3.49	4.23	0.44	0.18	1.32
74	3.36	4.55	0.72	0.22	1.38
75	3.14	3.92	1.33	0.13	1.01
76	3.66	4.41	0.50	0.19	1.29
77	3.36	4.45	0.52	0.20	1.30
78	3.28	4.34	0.71	0.19	1.25
79	3.34	4.33	0.43	0.19	1.31
80	3.33	4.21	0.63	0.18	1.28
81	3.36	4.28	0.78	0.19	1.31
82	3.59	4.36	0.49	0.19	1.37
83	3.17	3.99	1.68	0.14	0.99
84	3.37	4.31	1.11	0.18	1.20
85	3.10	4.50	2.17	0.20	1.15
86	3.07	3.73	0.53	0.13	0.89
87	3.16	4.06	1.73	0.15	1.11
88	3.14	3.97	1.86	0.13	1.01
89	3.31	3.92	0.42	0.15	1.06
90	3.59	4.23	0.53	0.18	1.28

Table 4. Chemistry of major elements—Continued

[In percent by weight]

Sample site number	Na[1]	K[2]	Ca[2]	Ti[2]	Fe[1]
91	3.29	4.08	1.06	0.16	1.23
92	3.47	4.23	0.59	0.17	1.28
93	3.44	4.48	1.74	0.22	1.42
94	3.54	4.71	0.59	0.24	1.50
95	3.58	4.60	0.84	0.23	1.56
96	3.59	4.62	0.87	0.24	1.62
97	3.66	4.63	0.84	0.23	1.55
98	3.01	3.69	0.87	0.10	0.88
99	3.31	4.32	0.66	0.17	1.18
100	3.46	4.49	0.57	0.20	1.27
101	3.41	4.19	0.49	0.18	1.28
102	3.22	4.16	1.28	0.17	1.20
103	3.19	3.54	0.32	0.11	0.87
104	3.02	3.61	1.00	0.10	0.84
105	3.18	3.75	0.27	0.12	0.95
106	3.06	3.76	1.07	0.12	0.85
107	3.19	3.85	2.55	0.13	0.96
108	3.34	3.73	0.34	0.11	0.96
110	3.08	3.83	0.66	0.12	0.85
111	3.41	4.27	0.48	0.19	1.23
112	3.29	4.34	1.00	0.19	1.26
113	3.29	4.06	0.50	0.18	1.23
114	3.16	4.44	1.37	0.13	0.98
115	3.34	3.97	1.36	0.14	1.10
116	3.48	4.54	0.85	0.20	1.26
117	3.21	3.81	0.31	0.13	0.95
118	3.35	4.52	2.18	0.19	1.19
119	3.14	3.74	0.29	0.12	0.92
120	3.50	4.37	0.77	0.18	1.22
121	3.46	4.45	0.48	0.19	1.33
122	3.50	3.97	0.32	0.13	1.09
123	3.58	4.41	0.57	0.22	1.42
124	2.94	3.64	0.55	0.11	0.89
125	3.06	3.72	0.51	0.12	0.84
126	2.98	3.59	0.42	0.11	0.81
127	2.92	4.12	2.85	0.14	0.97
128	3.16	3.99	0.42	0.15	1.12
129	3.15	4.16	0.38	0.17	1.12
130	3.23	4.36	0.48	0.19	1.21
131	3.10	4.16	0.54	0.18	1.11
132	3.28	4.86	1.50	0.35	1.58
133	3.34	4.87	1.23	0.33	1.55
134	3.33	4.48	0.79	0.22	1.61
135	3.21	4.50	0.74	0.21	1.24
136	3.17	4.34	0.63	0.18	1.12

Table 4. Chemistry of major elements—Continued

[In percent by weight]

Sample site number	Na[1]	K[2]	Ca[2]	Ti[2]	Fe[1]
137	3.12	4.14	0.50	0.17	1.08
138	3.20	4.58	0.71	0.22	1.27
139	3.13	4.10	0.96	0.16	0.98
140	3.24	4.29	0.84	0.19	1.12
141	3.17	4.17	1.11	0.16	1.11
142	3.12	3.98	0.40	0.15	1.01
143	3.00	4.12	1.27	0.16	1.00
144	3.01	3.62	0.34	0.11	0.85
145	3.03	3.99	0.62	0.15	1.01
146	3.37	4.18	0.51	0.16	1.12
147	3.30	4.21	0.42	0.16	1.17
148	3.06	3.81	0.41	0.12	0.94
149	3.15	4.21	0.72	0.17	1.11
150	3.01	3.92	0.99	0.14	0.94
151	3.10	4.08	0.71	0.16	1.05
152	3.00	4.14	0.91	0.15	0.97
153	3.25	4.07	0.40	0.14	1.03
154	3.04	4.06	1.77	0.16	1.05
155	3.04	4.00	1.08	0.15	1.04
156	3.08	4.12	0.90	0.16	1.04
157	3.46	3.95	0.76	0.15	1.22
158	3.40	3.97	0.84	0.14	1.18
159	3.65	3.99	0.92	0.15	1.29

[1]Neutron activation.
[2]X-ray fluorescence.

Table 5. Chemistry of common trace elements in the Tiva Canyon Tuff

[In ppm by weight; <, less than]

Sample site number	Sc[1]	Rb[1]	Rb[2]	Sr[2]	Y[2]	Zr[2]	Nb[2]	Cs[1]	Ba[1]	Ba[2]	Hf[1]	Th[1]	U[1]
1	4.7	110	126	150	45	582	19	2	1,700	1,801	13	20	3.7
2	5.0	100	107	215	38	640	17	2	2,100	2,484	13	17	2.5
3	5.0	120	121	167	42	588	17	2	1,700	1,887	13	18	4.2
4	4.8	120	127	150	41	547	17	2	1,800	1,798	12	18	4.9
5	4.7	120	129	158	41	578	20	2	1,800	1,818	12	20	3.5
6	5.0	100	118	181	45	616	17	2	2,000	2,162	13	18	3.7
7	5.0	98	114	184	44	642	20	3	1,900	2,066	12	18	2.6
8	4.6	100	110	178	40	619	18	2	1,700	2,021	12	17	3.1
9	4.8	120	113	178	39	609	17	1	2,000	2,133	13	18	3.5
10	4.7	100	120	161	40	560	18	2	1,600	1,776	12	19	3.9
11	5.1	110	111	170	39	634	17	2	1,800	2,012	13	18	3.3
12	4.6	95	112	179	39	580	18	2	1,700	2,057	12	18	3.2
13	6.4	66	77	236	37	787	9	<1	2,400	2,703	14	14	<0.5
14	4.6	110	124	158	39	566	19	2	1,600	1,822	13	19	4.1
15	5.0	78	119	86	42	601	19	1	700	695	13	19	4.2
16	4.6	95	122	158	37	554	17	1	1,700	1,805	12	20	4.1
17	4.1	81	128	123	40	507	19	<1	1,200	1,363	12	20	3.9
18	4.3	100	121	147	39	517	19	2	1,600	1,756	12	19	3.4
19	6.3	60	87	195	38	755	13	<1	1,900	2,154	14	16	2.8
20	5.0	110	115	169	37	594	20	2	1,800	1,995	13	18	3.1
21	6.7	110	96	194	39	820	12	<1	2,200	2,377	15	18	2.6
22	5.1	95	117	160	38	575	19	2	1,800	1,959	13	18	3.7
23	6.0	100	104	111	40	620	17	1	1,000	1,048	14	19	3.3
24	7.4	75	94	188	40	779	12	<1	2,100	2,202	15	16	2.4
25	6.5	70	83	200	35	646	10	3	1,700	1,796	13	15	3.3
26	5.3	92	103	113	38	613	16	2	1,100	1,146	13	19	2.8
27	6.1	92	106	94	42	612	18	2	1,100	1,038	13	17	1.7
28	5.4	79	113	102	40	602	20	2	1,100	1,081	13	19	3.9
29	5.8	75	98	143	36	659	15	<1	1,700	1,507	15	20	3.4
30	4.6	95	119	75	43	528	18	2	690	696	13	21	3.9
31	4.9	130	121	76	40	517	18	3	670	612	13	22	3.9
32	5.0	83	129	75	43	588	21	2	700	733	14	22	3.7

Table 5. Chemistry of common trace elements in the Tiva Canyon Tuff—Continued

[In ppm by weight; <, less than]

Sample site number	Sc[1]	Rb[1]	Rb[2]	Sr[2]	Y[2]	Zr[2]	Nb[2]	Cs[1]	Ba[1]	Ba[2]	Hf[1]	Th[1]	U[1]
33	6.3	120	110	100	38	591	16	1	1,000	1,050	14	20	3.9
34	5.5	130	122	70	44	532	21	2	640	672	14	22	3.7
35	5.9	89	103	140	34	545	15	2	850	872	14	19	3.5
36	5.2	150	143	61	44	503	22	3	540	509	13	22	4.5
37	5.1	130	131	62	43	502	22	2	560	564	13	22	4.4
38	5.7	130	108	91	41	595	17	2	960	885	13	21	3.7
39	3.9	140	142	53	43	455	23	3	530	415	12	22	3.9
40	6.3	110	132	101	45	644	18	2	1,000	1,035	15	20	3.7
41	5.8	100	115	100	41	578	16	2	890	950	15	20	3.1
42	6.7	110	110	103	44	637	17	2	1,100	1,049	15	20	4.0
43	6.2	110	112	110	41	624	17	2	1,000	997	14	20	3.1
44	5.0	130	119	83	38	502	19	2	•660	591	13	21	3.7
45	4.5	110	131	61	43	489	23	<1	460	500	12	22	3.4
46	6.0	120	118	104	48	620	18	3	820	934	14	19	3.3
47	5.0	110	139	63	44	513	22	3	530	545	13	22	3.9
48	8.4	68	97	166	42	790	14	<1	2,200	2,013	17	19	2.5
50	5.2	140	135	63	43	529	21	3	600	605	14	24	4.1
51	1.6	170	181	23	36	199	30	2	180	76	9	26	6.2
52	5.3	110	116	85	41	538	19	2	850	750	14	20	3.3
53	5.0	120	133	89	43	535	22	3	780	684	13	21	3.1
54	1.7	170	186	22	39	200	31	3	170	72	9	27	5.3
55	5.2	120	110	97	36	529	17	2	770	717	14	20	3.5'
56	4.0	160	151	50	44	366	25	3	410	316	12	25·	5.0
57	4.8	120	137	72	44	462	21	2	590	545	12	22	5.0
58	4.9	130	144	58	43	475	24	3	550	513	14	25	5.5
59	5.8	120	128	73	44	547	22	2	770	703	14	22	4.2
60	6.0	110	127	99	40	613	18	1	990	1,005	14	23	3.9
61	4.9	120	127	70	44	511	21	2	710	625	13	23	5.0
62	4.0	120	140	51	43	444	23	3	580	453	13	24	4.4
63	2.8	150	163	44	44	341	28	3	240	243	11	25	4.4
64	6.2	120	116	93	42	603	18	2	890	897	15	21	3.0
65	5.5	110	117	82	41	551	19	2	720	675	13	21	3.5
66	6.6	100	107	100	42	629	18	1	890	1,040	15	20	3.8
67	5.5	120	117	95	44	595	20	2	890	897	14	21	3.9

[In ppm by weight; <, less than]

Sample site number	Sc[1]	Rb[1]	Rb[2]	Sr[2]	Y[2]	Zr[2]	Nb[2]	Cs[1]	Ba[1]	Ba[2]	Hf[1]	Th[1]	U[1]
68	5.6	77	103	120	39	647	16	1	1,200	1,168	13	17	3.1
69	4.7	91	126	64	43	519	20	2	620	589	13	22	4.1
70	4.2	110	131	55	41	463	22	2	530	484	12	23	4.4
71	3.4	140	147	52	40	388	22	3	390	339	11	23	4.5
72	1.8	170	189	14	43	209	31	3	110	72	9	28	4.7
73	4.7	150	142	57	43	452	23	3	420	466	13	24	4.9
74	5.3	120	121	72	45	577	19	2	730	678	14	22	4.5
75	2.8	160	160	51	38	315	26	3	300	212	11	25	4.9
76	5.1	130	138	61	45	506	20	2	730	555	14	24	4.5
77	4.4	120	139	62	44	480	22	2	490	500	12	23	4.6
78	4.5	110	127	71	42	520	21	2	650	601	13	22	3.7
79	4.5	96	138	59	40	506	21	2	560	547	13	23	4.1
80	4.7	150	136	59	42	476	23	2	430	484	12	23	4.0
81	4.3	110	131	65	42	477	22	2	520	540	13	23	4.5
82	4.9	140	135	68	43	499	24	3	660	566	14	24	4.2
83	3.1	150	153	53	38	332	26	3	290	245	11	25	6.0
84	4.4	130	135	71	47	470	23	3	580	485	13	23	5.0
85	4.4	76	122	84	40	491	20	2	660	634	12	20	3.7
86	2.4	130	165	38	41	313	28	2	260	179	11	25	5.4
87	3.5	140	146	59	39	380	25	3	390	329	11	22	3.9
88	2.9	150	149	64	41	325	25	3	270	229	11	25	4.8
89	3.6	130	151	47	43	391	23	3	350	336	12	24	4.9
90	4.8	110	140	61	47	476	22	3	700	499	14	23	3.8
91	3.7	120	141	58	40	420	22	2	460	416	12	23	5.2
92	5.2	120	134	61	42	475	23	3	580	510	13	23	4.1
93	5.9	100	102	103	40	550	15	2	910	846	14	20	2.9
94	6.5	79	101	112	42	660	17	2	1,200	1,140	15	20	4.5
95	6.0	96	104	104	43	620	18	2	960	945	15	19	4.1
96	6.4	90	99	103	41	625	18	2	1,100	1,022	15	20	3.2
97	6.5	110	114	103	42	631	20	2	990	952	15	20	2.7
98	1.9	160	172	46	41	246	30	3	240	226	10	26	5.0
99	4.1	110	144	57	44	442	26	3	370	419	13	23	3.9
100	5.0	130	133	67	43	536	23	3	560	587	14	22	2.8
101	4.9	130	134	61	47	496	22	2	520	503	12	22	3.8

Table 5. Chemistry of common trace elements in the Tiva Canyon Tuff—Continued

[In ppm by weight; <, less than]

Sample site number	Sc[1]	Rb[1]	Rb[2]	Sr[2]	Y[2]	Zr[2]	Nb[2]	Cs[1]	Ba[1]	Ba[2]	Hf[1]	Th[1]	U[1]
102	4.1	140	145	60	44	445	25	2	430	386	12	23	4.6
103	2.1	160	176	36	43	260	31	2	220	153	10	26	4.9
104	1.9	150	177	36	39	239	32	2	150	131	9	24	4.5
105	2.5	150	176	32	45	295	29	3	180	164	10	26	5.3
106	2.3	140	166	43	41	297	30	2	190	173	10	24	4.3
107	3.0	130	144	70	39	327	25	3	220	206	10	23	6.1
108	2.3	170	172	45	43	285	27	3	250	193	11	25	5.1
110	2.3	140	168	41	40	280	29	3	300	163	10	24	4.9
111	4.8	130	130	74	43	493	20	2	630	614	12	23	2.8
112	4.8	120	131	74	40	500	22	2	560	590	12	22	4.0
113	4.5	120	137	63	40	471	22	2	470	480	12	22	4.8
114	2.9	160	162	53	40	310	27	3	240	225	11	23	5.0
115	3.3	150	160	60	41	340	25	3	300	223	11	25	5.5
116	5.1	110	138	83	41	541	21	2	700	691	13	23	4.0
117	2.7	170	165	35	40	328	29	2	520	223	10	26	5.2
118	4.9	130	135	77	41	465	22	2	560	535	13	22	4.2
119	2.6	160	169	30	39	303	29	3	220	174	10	25	4.9
120	4.4	140	139	62	42	475	23	3	570	502	13	23	4.6
121	5.3	130	136	65	44	530	20	2	650	582	14	22	3.6
122	3.4	170	170	42	42	360	26	2	430	265	12	27	5.6
123	5.9	130	124	73	41	532	19	2	750	676	14	22	4.6
124	2.1	160	171	52	42	248	30	3	230	210	10	26	4.3
125	2.1	150	174	38	39	292	31	3	150	163	9	24	5.2
126	1.9	160	169	49	41	268	30	3	220	177	9	23	4.0
127	2.5	140	155	77	40	343	26	3	260	242	9	22	4.5
128	3.3	140	152	47	45	374	25	3	450	316	11	23	4.2
129	3.7	130	148	50	34	427	24	3	450	386	11	23	4.0
130	4.0	110	137	59	47	490	23	2	430	465	12	21	3.4
131	3.8	120	139	57	43	453	25	3	470	462	11	20	4.3
132	7.0	80	82	230	38	821	12	2	2,400	2,836	14	14	2.6
133	6.8	88	86	227	37	831	10	<1	2,300	2,738	15	15	1.7
134	6.3	110	124	67	39	538	20	3	730	589	16	24	3.8
135	4.8	94	112	76	38	533	18	2	640	681	12	18	2.9
136	4.0	100	138	65	42	469	23	2	490	494	12	21	3.4

Table 5. Chemistry of common trace elements in the Tiva Canyon Tuff—Continued

[In ppm by weight; <, less than]

Sample site number	Sc[1]	Rb[1]	Rb[2]	Sr[2]	Y[2]	Zr[2]	Nb[2]	Cs[1]	Ba[1]	Ba[2]	Hf[1]	Th[1]	U[1]
137	3.9	83	139	55	40	431	23	3	430	414	11	21	3.7
138	5.1	96	114	76	38	577	17	2	800	730	12	18	3.4
139	3.5	110	147	62	42	421	24	3	350	361	11	21	3.6
140	4.1	130	138	67	42	477	23	2	480	488	11	21	3.2
141	3.7	140	143	64	44	426	23	3	390	383	10	22	4.0
142	3.2	120	149	46	42	376	24	2	330	291	11	23	4.4
143	3.2	130	146	60	36	374	24	3	340	315	10	22	3.8
144	1.8	150	175	46	45	285	31	2	220	179	10	24	4.2
145	3.2	110	147	51	40	368	25	3	380	321	10	22	4.5
146	3.3	140	157	55	45	430	26	3	410	326	12	23	5.3
147	3.5	140	155	49	40	405	25	2	370	321	11	24	4.1
148	2.5	140	166	44	43	323	25	3	230	208	11	23	4.6
149	3.8	120	150	60	42	454	24	3	440	421	11	21	4.2
150	2.9	130	151	62	39	375	26	3	310	290	10	21	4.1
151	3.7	120	149	51	40	415	24	2	460	343	11	23	4.5
152	3.1	130	153	58	41	366	25	3	360	317	11	22	3.9
153	3.0	140	154	46	40	390	26	2	400	294	12	23	4.4
154	3.1	130	149	68	39	389	23	3	350	311	11	21	3.6
155	3.2	140	148	53	39	366	24	2	370	319	10	22	3.9
156	3.3	130	148	60	41	388	25	3	420	348	11	22	4.4
157	3.3	170	154	53	42	362	26	3	350	265	13	28	6.3
158	3.5	140	150	54	39	366	24	3	330	265	13	27	5.9
159	3.9	160	145	71	41	380	25	3	290	323	12	28	6.3

[1]Neutron activation.
[2]X-ray fluorescence.

Table 6. Chemistry of rare earth elements in the Tiva Canyon Tuff

[In ppm by weight; <, less than]

Sample site number	La[1]	La[2]	Ce[1]	Ce[2]	Nd[1]	Sm[1]	Eu[1]	Tb[1]	Yb[1]	Lu[1]
1	150	152	250	251	82	11	2.8	1.1	3.4	0.50
2	160	139	270	282	88	11	3.2	0.9	3.0	0.38
3	140	148	250	258	75	11	2.9	1.4	3.4	0.46
4	150	151	260	261	81	11	2.9	1.3	3.5	0.48
5	150	146	250	249	91	11	3.0	1.0	3.5	0.46
6	150	171	260	279	91	11	3.1	1.4	3.7	0.51
7	160	165	270	279	87	11	3.1	1.3	3.5	0.51
8	160	169	260	277	83	11	3.0	1.0	3.2	0.44
9	160	153	270	275	90	11	3.2	1.0	3.3	0.47
10	140	144	250	238	82	11	2.8	1.0	3.1	0.46
11	160	180	280	292	93	11	3.0	1.0	3.4	0.42
12	140	151	250	263	80	10	2.8	1.2	3.0	0.43
13	210	229	360	383	120	13	4.2	1.4	2.7	0.42
14	140	156	260	252	85	10	2.9	1.1	3.2	0.46
15	170	192	300	302	98	13	2.4	1.4	3.5	0.51
16	150	149	250	254	80	10	2.8	1.4	3.4	0.46
17	120	134	210	224	75	9	2.2	1.4	3.2	0.43
18	140	138	240	240	78	10	2.6	1.0	3.4	0.43
19	210	228	360	372	120	13	3.8	0.9	3.1	0.47
20	160	156	270	267	91	13	3.1	1.2	2.7	0.46
21	230	251	410	406	130	15	4.3	1.2	3.2	0.44
22	160	153	270	272	91	11	3.1	1.2	3.3	0.46
23	190	207	340	314	110	16	3.0	1.2	3.2	0.56
24	240	231	420	386	140	18	4.6	1.2	3.1	0.58
25	210	209	360	334	130	16	3.8	1.2	3.0	0.47
26	180	212	310	329	110	13	3.0	1.5	3.3	0.48
27	200	206	330	331	120	17	3.3	1.1	3.0	0.48
28	180	220	320	330	95	13	2.8	1.4	3.7	0.48
29	200	217	360	340	120	14	3.4	1.2	3.4	0.49
30	150	178	280	277	94	12	2.2	1.5	3.7	0.48
31	160	187	290	284	100	13	2.2	1.5	3.9	0.50
32	170	195	310	306	110	13	2.5	1.5	3.8	0.52
33	200	198	360	317	130	17	3.3	1.1	3.3	0.58
34	180	189	330	285	120	17	2.7	1.4	3.8	0.57
35	200	199	360	301	120	16	3.0	1.1	3.4	0.60
36	150	158	290	264	100	16	2.3	1.2	4.1	0.58
37	160	160	290	245	100	15	2.3	1.5	3.8	0.61
38	190	202	350	317	110	17	3.0	1.5	3.9	0.56
39	120	131	230	212	85	13	1.8	1.1	3.9	0.58
40	210	234	380	346	130	18	3.5	1.2	3.8	0.61
41	180	198	330	290	120	16	2.9	1.3	3.5	0.56
42	220	215	400	341	120	18	3.5	1.6	3.9	0.59
43	200	205	360	314	120	18	2.9	1.0	3.7	0.61
44	160	173	290	271	100	15	2.2	1.1	3.6	0.61
45	140	176	260	270	96	15	2.2	1.4	3.6	0.59

Table 6. Chemistry of rare earth elements in the Tiva Canyon Tuff—Continued

[In ppm by weight; <, less than]

Sample site number	La[1]	La[2]	Ce[1]	Ce[2]	Nd[1]	Sm[1]	Eu[1]	Tb[1]	Yb[1]	Lu[1]
46	180	208	330	318	110	17	3.0	1.5	3.4	0.57
47	150	173	280	259	96	15	2.2	1.3	3.6	0.57
48	260	223	460	368	160	20	4.7	1.2	3.6	0.59
50	160	172	300	279	110	16	2.5	1.5	3.9	0.58
51	33	53	74	83	30	7	0.3	1.3	3.8	0.51
52	170	177	310	281	100	16	2.6	1.4	3.7	0.62
53	160	177	290	269	99	15	2.4	1.2	3.6	0.59
54	35	57	80	70	30	8	0.5	1.0	4.0	0.57
55	180	178	320	276	120	16	2.7	1.2	3.3	0.59
56	100	106	210	172	76	13	1.6	1.2	4.3	0.68
57	150	152	280	238	100	15	2.2	1.5	3.7	0.64
58	150	158	290	253	98	15	2.4	1.7	4.5	0.65
59	190	198	350	296	130	17	2.9	1.2	4.3	0.65
60	210	192	370	314	130	18	3.3	1.7	3.9	0.64
61	160	184	300	271	97	13	2.2	1.7	4.1	0.56
62	130	151	250	238	77	12	1.9	1.5	4.1	0.55
63	71	88	140	144	53	9	1.0	1.4	4.1	0.53
64	200	195	350	307	130	18	3.1	0.8	4.0	0.57
65	190	217	340	326	110	14	2.6	1.5	3.8	0.52
66	210	234	400	342	140	19	3.6	1.4	3.8	0.59
67	180	187	320	306	110	14	2.7	1.7	4.0	0.60
68	180	210	310	329	94	13	2.9	1.2	3.6	0.47
69	150	178	280	257	97	13	2.2	1.3	4.2	0.57
70	130	154	240	241	86	12	1.9	1.4	4.1	0.55
71	100	133	190	198	68	10	1.3	1.1	3.9	0.54
72	35	46	81	78	31	8	0.4	0.9	4.3	0.62
73	140	155	250	225	94	15	2.0	1.3	4.4	0.63
74	170	185	310	275	110	14	2.5	1.4	4.2	0.58
75	74	104	150	152	51	9	0.9	1.2	4.2	0.54
76	160	171	300	266	110	16	2.4	1.6	4.1	0.62
77	130	150	250	230	85	12	1.9	1.5	4.0	0.56
78	150	171	270	272	90	12	2.2	1.0	4.0	0.55
79	150	169	280	266	94	12	2.1	1.3	4.1	0.54
80	140	164	260	240	93	14	2.0	1.6	3.7	0.58
81	140	160	260	240	87	12	2.0	1.4	4.1	0.56
82	150	154	280	251	97	13	2.1	1.7	4.4	0.56
83	82	101	170	163	61	10	1.0	1.4	4.1	0.55
84	140	153	270	233	100	16	2.2	1.5	4.3	0.69
85	140	164	260	246	89	14	2.1	1.1	3.3	0.54
86	63	87	130	134	46	8	0.7	1.4	4.1	0.53
87	100	113	200	178	70	12	1.5	1.2	3.9	0.55
88	78	96	150	151	53	9	1.0	1.2	4.0	0.52
89	100	131	190	186	72	10	1.4	1.3	4.2	0.56
90	150	158	270	246	97	16	2.2	1.4	4.2	0.67
91	120	134	220	204	74	11	1.7	1.2	4.1	0.57

Table 6. Chemistry of rare earth elements in the Tiva Canyon Tuff—Continued

[In ppm by weight; <, less than]

Sample site number	La[1]	La[2]	Ce[1]	Ce[2]	Nd[1]	Sm[1]	Eu[1]	Tb[1]	Yb[1]	Lu[1]
92	160	173	300	263	110	16	2.3	1.2	4.0	0.62
93	180	189	330	279	120	17	3.0	1.1	3.8	0.61
94	200	216	370	328	130	18	3.3	1.5	3.4	0.56
95	200	193	360	320	120	18	3.2	1.6	3.5	0.60
96	210	225	370	351	130	18	3.4	1.7	3.3	0.55
97	200	207	370	325	130	18	3.1	<0.5	3.6	0.62
98	41	45	91	84	42	9	0.5	1.1	4.2	0.60
99	130	146	240	217	80	14	1.6	1.3	4.0	0.61
100	160	190	300	283	110	16	2.3	<0.5	3.8	0.61
101	150	158	270	230	100	15	2.1	1.5	4.0	0.63
102	120	134	230	214	87	13	1.6	1.5	3.9	0.59
103	46	59	100	105	39	9	0.6	1.4	3.9	0.57
104	37	55	81	67	31	8	0.5	<0.5	3.6	0.49
105	54	69	120	101	51	10	0.7	1.5	4.4	0.65
106	56	69	120	114	45	10	0.8	1.3	4.0	0.61
107	75	85	150	135	54	11	1.1	1.2	3.9	0.56
108	56	69	120	112	49	10	0.8	1.1	4.0	0.61
110	54	63	120	105	38	10	0.6	1.4	4.0	0.57
111	150	168	290	256	100	16	2.3	1.5	3.9	0.64
112	150	162	280	276	90	15	2.4	1.3	3.8	0.54
113	140	157	270	241	97	14	2.0	<0.5	4.2	0.66
114	77	91	160	140	63	11	1.1	<0.5	4.1	0.56
115	88	89	180	150	66	12	1.1	1.5	4.3	0.64
116	160	170	310	262	110	16	2.5	<0.5	4.0	0.63
117	75	99	150	152	57	11	1.0	1.3	4.1	0.62
118	150	152	280	253	98	15	2.2	1.5	4.0	0.59
119	68	85	140	143	48	10	0.8	1.0	4.3	0.58
120	140	157	270	245	100	15	2.0	1.2	4.2	0.61
121	170	177	320	271	120	16	2.6	1.5	4.1	0.63
122	91	106	190	177	67	12	1.3	<0.5	4.5	0.68
123	180	185	340	289	110	17	2.6	<0.5	4.1	0.61
124	42	53	100	92	39	9	0.5	1.0	4.2	0.54
125	52	70	110	109	40	8	0.7	1.1	3.4	0.49
126	42	63	88	108	34	7	0.5	1.1	3.6	0.50
127	69	93	130	147	47	9	0.9	1.0	3.6	0.46
128	93	113	170	177	64	10	1.3	1.3	3.6	0.51
129	91	100	220	234	54	8	1.4	1.0	3.0	0.44
130	130	170	240	251	82	12	1.8	1.4	3.5	0.52
131	120	150	220	235	76	11	1.6	1.1	3.6	0.46
132	240	230	400	389	130	15	4.5	1.3	2.7	0.42
133	240	240	400	388	120	15	4.5	1.2	2.8	0.37
134	200	196	340	295	120	15	2.7	1.2	4.2	0.60
135	160	199	290	297	88	13	2.3	1.2	3.2	0.43
136	130	158	230	232	74	11	1.7	1.2	3.5	0.48
137	120	144	210	226	71	11	1.5	1.4	3.6	0.47

Table 6. Chemistry of rare earth elements in the Tiva Canyon Tuff—Continued

[In ppm by weight; <, less than]

Sample site number	La[1]	La[2]	Ce[1]	Ce[2]	Nd[1]	Sm[1]	Eu[1]	Tb[1]	Yb[1]	Lu[1]
138	170	200	280	313	93	12	2.2	1.3	3.1	0.47
139	110	138	190	220	60	10	1.4	1.3	3.5	0.48
140	130	162	230	238	74	12	1.9	1.2	3.6	0.48
141	110	140	200	220	66	11	1.5	1.0	3.9	0.49
142	88	113	170	183	52	10	1.1	1.4	3.7	0.49
143	90	121	170	193	53	9	1.2	1.4	3.5	0.44
144	41	54	90	95	30	8	0.5	1.4	3.6	0.47
145	89	111	170	165	60	9	1.0	1.0	3.3	0.44
146	98	135	180	191	66	11	1.3	1.3	4.0	0.53
147	100	112	180	178	65	10	1.4	1.3	3.9	0.51
148	64	90	130	140	47	10	0.8	1.3	3.7	0.54
149	120	159	210	247	73	11	1.5	1.1	3.8	0.49
150	85	107	150	171	54	9	1.0	1.3	3.7	0.47
151	100	133	190	192	62	10	1.3	1.1	3.7	0.50
152	91	125	160	197	50	9	1.1	1.2	3.6	0.46
153	93	110	170	175	61	10	1.2	1.3	3.8	0.50
154	92	110	170	182	61	10	1.1	1.2	3.7	0.49
155	92	107	170	175	57	10	1.1	1.3	3.5	0.49
156	97	115	180	183	58	10	1.3	1.3	4.0	0.50
157	93	108	190	167	67	11	1.3	1.3	4.3	0.59
158	93	106	190	170	67	11	1.5	1.5	4.2	0.54
159	110	120	230	177	72	12	1.6	1.7	4.7	0.62

[1]Neutron activation.
[2]X-ray fluorescence.
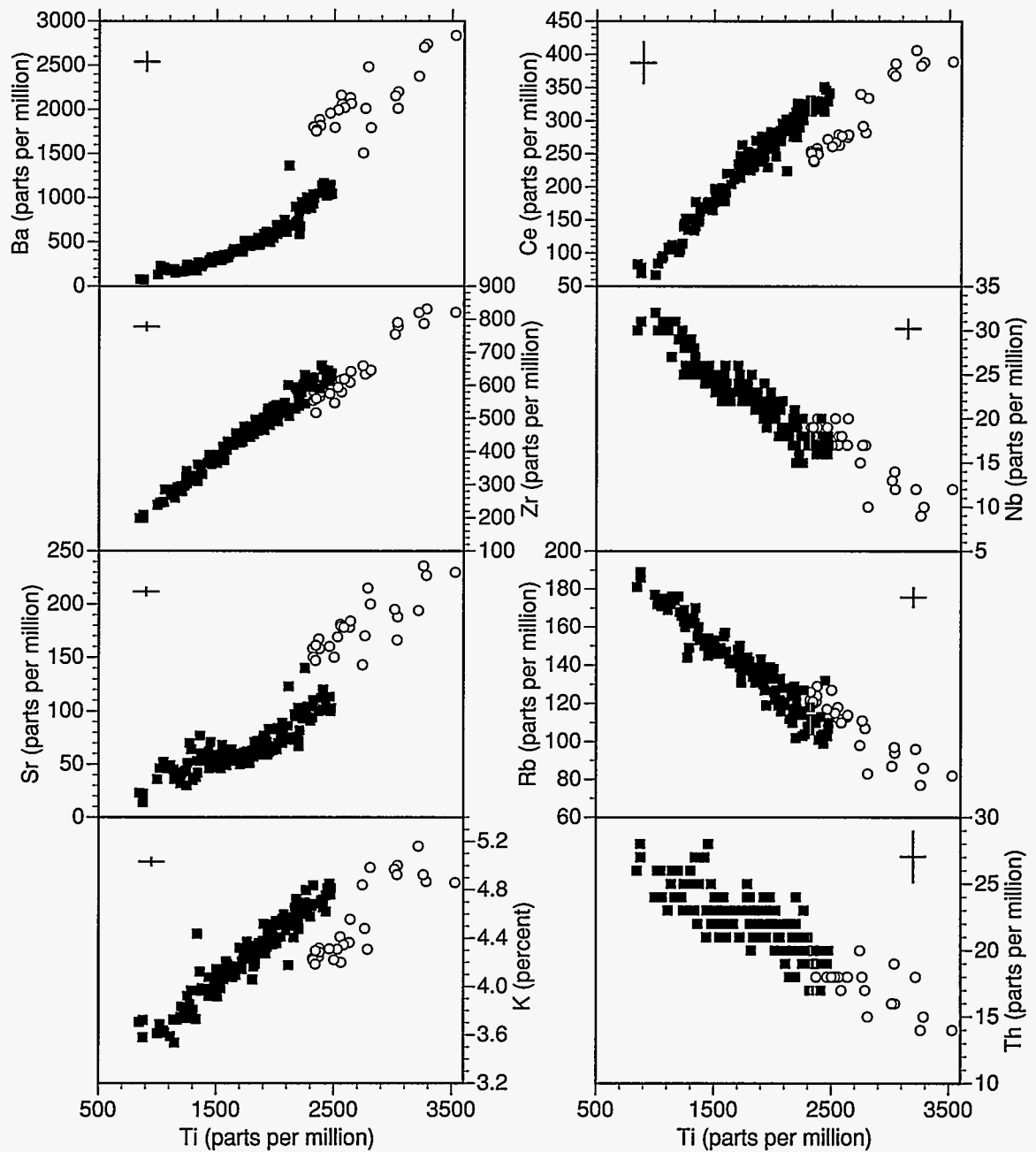
Figure 12. Variations of barium, cerium, zirconium, niobium, strontium, rubidium, potassium, and thorium concentrations as a function of titanium concentration in the Tiva Canyon Tuff upper cliff and caprock samples. The open symbols are caprock samples; the filled symbols are samples of upper cliff. The trends in these elements are typical of differentiation in magmatic systems, although the caprock trends are more diffuse. Typical 2σ errors are shown by the crosses.
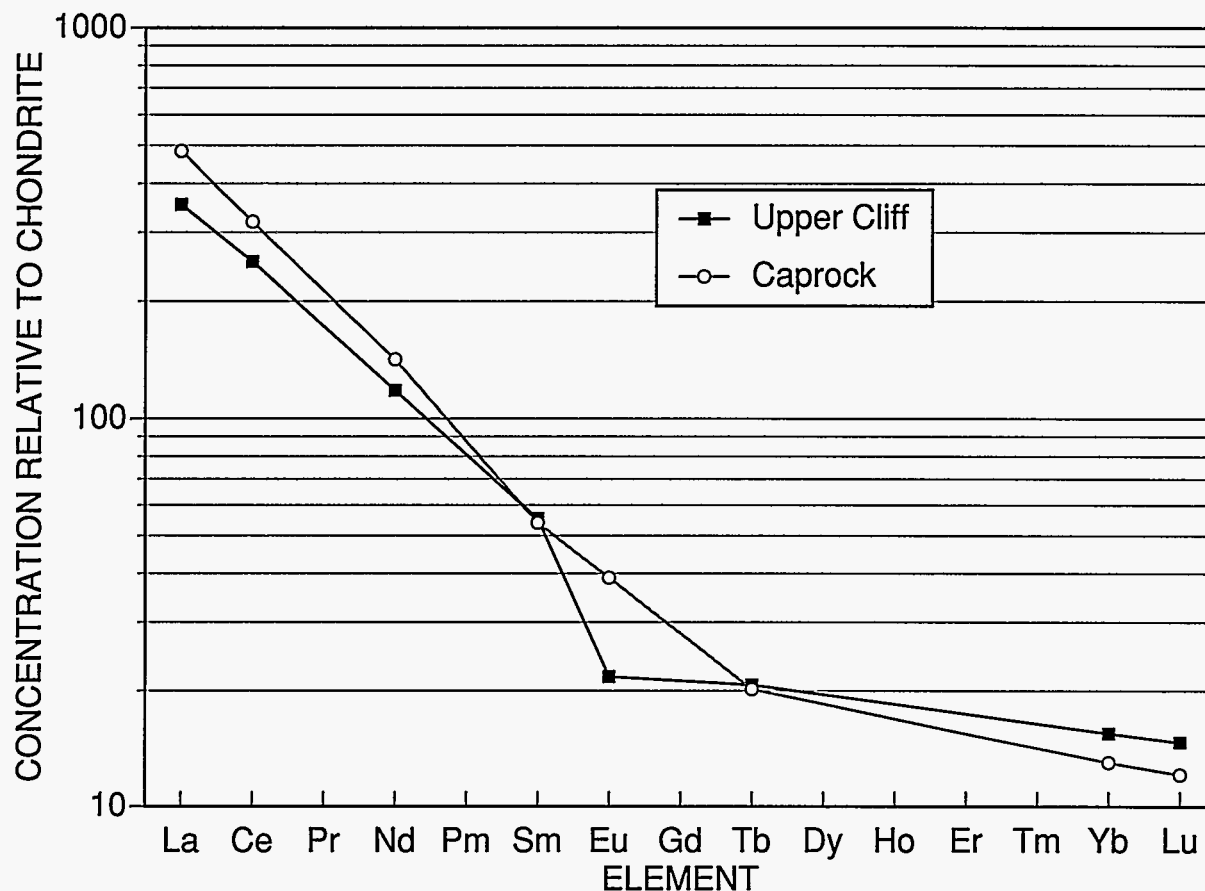
Figure 13. Average rare earth element concentrations (normalized to chondritic [Taylor and McClennan, 1985]) of the upper cliff (filled symbols) and caprock (open symbols) samples. The enrichment in light rare earth elements is typical of felsic igneous rocks. The only element showing a significant difference between upper cliff and caprock is europium, presumably because of plagioclase fractionation. Although the average values for europium are different for upper cliff and caprock, the ranges of the individual analyses overlap.

elements do with titanium contents (fig. 14), indicating that these components do not solely reflect magmatic values. In particular, calcium and $\delta^{18}O$ values in samples from both zones vary the least systematically with titanium contents, similar to what was observed in samples from the Solitario Canyon section. The trend between calcium and titanium clearly shows the effect of the addition of secondary calcite. Unlike titanium, elements such as sodium, uranium and iron are easily mobilized by post-emplacement, water-rock interactions that could result in the variations shown in figure 14.

Certain elements such as arsenic, selenium, mercury, silver, gold, and copper have been used as pathfinder elements for epithermal precious-metal deposits (Levinson, 1980). For example, the epithermal gold deposit in Fluorspar Canyon near Beatty,

Nevada, has elevated arsenic, silver, and mercury contents that correlate directly with gold concentrations (Greybeck and Wallace, 1991). With few exceptions, however, both the concentrations of typical pathfinder elements and the precious metals themselves are characteristically low in the upper cliff and caprock zone samples (table 7). Selenium, silver, and mercury are below detection limits, and both arsenic and gold are only marginally higher than typical magmatic levels in siliceous igneous rocks (Connors and others, 1993).

Discussion of Results

The correlations of barium, cerium, zirconium, niobium, strontium, rubidium, potassium, and thorium with titanium in the upper cliff and caprock samples
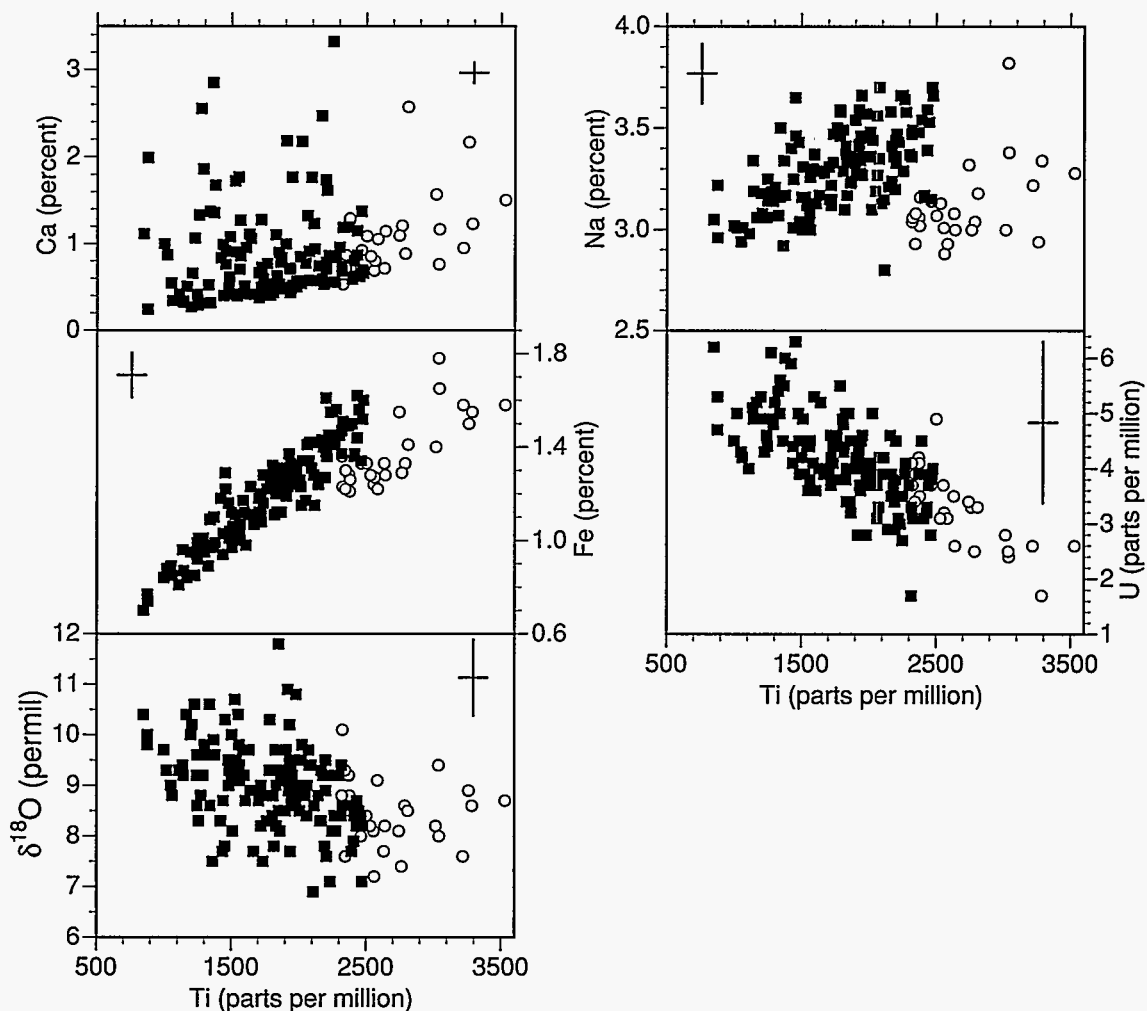
Figure 14. Variation of calcium, sodium, iron, and uranium concentrations and $\delta^{18}O$ as a function of titanium concentration in the upper cliff (filled symbols) and caprock (open symbols) zones. Note the large amount of scatter, especially in calcium and $\delta^{18}O$. This scatter is owing to post-eruptive processes. Typical 2σ errors are shown by the crosses.

result primarily from magmatic processes. Most of these correlations are also present in rocks of the Solitario Canyon reference section where the variations in each element can also be correlated with stratigraphic position. By analogy, the more extreme variations and poorer correlations with titanium contents for relatively mobile elements (calcium, sodium, iron, and uranium) imply that these elements do not record magmatic effects only, but vary because of secondary processes, such as low-temperature or deuteric alteration, in the same way that they did in samples from the Solitario Canyon reference section. The lack of high concentrations of pathfinder elements or significant variations in elements such as potassium,

rubidium, and strontium that are typically mobilized by high-temperature fluids, make hydrothermal alteration or epithermal mineralization of these samples highly unlikely.

As with the tuffs from the Solitario Canyon section, the $\delta^{18}O$ values of most samples from the upper cliff and caprock zones are higher than estimated original magmatic values and do not correlate with any of the elements measured in this study. Post-emplacement processes that can lead to ^{18}O enrichments in siliceous volcanic rocks include low-temperature hydration of glass, crystallization of quartz and feldspar from deuteric fluids, and addition of pedogenic carbonate and silica. The upper zones of

Table 7. Chemistry of uncommon trace elements

[All analyses by neutron activation in ppm by weight; <, less than; Au as ppb by weight; Se<3 ppm, Ag<5 ppm, Sn<100 ppm, Ir<5 ppb, and Hg<1 ppm]

Sample site number	Cr	Co	Ni	Zn	As	Br	Mo	Sb	Ta	W	Au
1	12	1	<22	79	2.5	<0.5	<1	0.4	1.1	<1	<2
2	<5	<1	<20	60	3.0	1.0	2	<0.1	<0.5	<1	4
3	7	3	<22	86	1.7	<0.5	<1	0.2	<0.5	<1	3
4	<5	<1	<21	84	1.0	<0.5	<1	0.3	<0.5	<1	<2
5	<5	<1	<22	100	1.4	<0.5	3	0.3	<0.5	<1	<2
6	<5	2	<23	<50	1.4	<0.5	<1	<0.1	<0.5	<1	<2
7	<5	<1	<22	80	1.4	<0.5	5	<0.1	<0.5	<1	<2
8	5	<1	<20	61	0.7	<0.5	<1	0.2	1.1	<1	<2
9	8	<1	<22	<50	<0.5	<0.5	<1	0.3	1.5	<1	3
10	<5	<1	<21	91	2.0	<0.5	<1	0.3	<0.5	<1	2
11	<5	2	<21	78	2.5	<0.5	<1	0.3	<0.5	<1	2
12	<5	<1	<20	<50	3.0	<0.5	<1	0.1	1.2	<1	<2
13	<5	3	<24	64	<0.5	<0.5	<1	<0.1	<0.5	<1	4
14	13	<1	<21	84	2.1	<0.5	5	0.4	<0.5	<1	<2
15	16	<1	<23	92	1.1	<0.5	<1	0.4	1.5	<1	<2
16	6	<1	<20	81	2.2	<0.5	4	0.2	1.1	<1	3
17	7	<1	<20	<50	1.8	<0.5	<1	0.2	1.6	<1	<2
18	<5	<1	<20	<50	2.2	<0.5	4	0.3	<0.5	<1	<2
19	<5	<1	<24	<50	2.1	<0.5	<1	<0.1	<0.5	<1	<2
20	11	1	<43	67	2.4	<0.5	<1	0.1	0.8	<1	<2
21	<5	<1	<27	<50	<0.5	<0.5	<1	<0.1	<0.5	<1	<2
22	<5	<1	<20	120	2.2	<0.5	4	<0.1	<0.5	<1	<2
23	11	2	<50	89	1.7	<0.5	<1	0.4	<0.5	<1	<2
24	<5	<1	<51	<50	2.4	<0.5	<1	<0.1	0.6	<1	<2
25	<5	1	<48	65	2.8	<0.5	<1	0.4	<0.5	<1	<2
26	7	2	<22	95	<0.5	<0.5	3	<0.1	1.2	<1	7
27	6	2	<46	87	2.4	<0.5	<1	<0.1	1.7	<1	<2
28	7	<1	220	110	1.6	<0.5	<1	<0.1	<0.5	<1	2
29	21	3	<24	100	2.3	<0.5	<1	0.3	<0.5	<1	3
30	11	<1	<21	86	2.4	<0.5	<1	0.3	<0.5	<1	<2
31	15	<1	<22	<50	2.1	<0.5	<1	0.2	1.4	<1	<2
32	13	3	<23	<50	3.2	<0.5	<1	<0.1	<0.5	<1	<2

Table 7. Chemistry of uncommon trace elements—Continued

[All analyses by neutron activation in ppm by weight; <, less than; Au as ppb by weight; Se<3 ppm, Ag<5 ppm, Sn<100 ppm, Ir<5 ppb, and Hg<1 ppm]

Sample site number	Cr	Co	Ni	Zn	As	Br	Mo	Sb	Ta	W	Au
33	6	<1	<28	80	2.9	<0.5	<1	0.6	<0.5	<1	<2
34	6	<1	<27	71	5.4	<0.5	4	<0.1	<0.5	<1	<2
35	8	3	<28	<50	3.1	<0.5	<1	0.5	<0.5	<1	<2
36	<5	<1	<26	100	2.6	<0.5	<1	0.4	<0.5	<1	<2
37	<5	3	<26	69	2.1	<0.5	<1	0.3	<0.5	<1	<2
38	<5	2	<28	<50	0.9	<0.5	<1	0.4	1.6	<1	<2
39	10	2	<24	90	1.4	<0.5	5	<0.1	<0.5	14	<2
40	8	<1	<29	87	1.2	<0.5	<1	0.6	1.6	<1	3
41	9	2	<29	<50	<0.5	<0.5	<1	<0.1	<0.5	<1	<2
42	<5	<1	<30	<50	1.5	<0.5	<1	0.3	<0.5	<1	<2
43	<5	3	<28	93	2.1	<0.5	3	0.3	1.4	<1	3
44	6	<1	<26	67	2.7	<0.5	<1	<0.1	<0.5	<1	<2
45	7	3	<38	<50	2.5	<0.5	<1	0.3	<0.5	<1	<2
46	<5	<1	<39	83	<0.5	<0.5	<1	<0.1	<0.5	<1	<2
47	7	4	<37	<50	2.1	<0.5	<1	<0.1	1.8	<1	<2
48	<5	3	<33	120	2.2	<0.5	<1	0.3	1.9	<1	<2
50	10	<1	<39	<50	1.6	<0.5	<1	<0.1	<0.5	<1	<2
51	12	2	<27	110	5.6	<0.5	<1	0.4	<0.5	<1	<2
52	8	<1	<39	<50	2.8	<0.5	<1	0.2	<0.5	<1	<2
53	<5	<1	<40	<50	2.7	<0.5	<1	<0.1	<0.5	<1	<2
54	8	1	<21	61	5.8	<0.5	<1	0.2	1.9	<1	3
55	5	3	<28	<50	3.3	<0.5	<1	0.4	<0.5	<1	6
56	9	3	<27	<50	2.7	<0.5	4	0.5	1.7	<1	<2
57	7	3	<38	<50	3.4	<0.5	<1	0.3	<0.5	<1	16
58	9	<1	<29	<50	2.8	<0.5	<1	0.3	<0.5	<1	<2
59	<5	3	<30	130	1.9	<0.5	<1	1.9	1.9	<1	<2
60	<5	2	<30	77	1.3	<0.5	<1	<0.1	<0.5	<1	<2
61	13	2	<21	100	1.4	<0.5	<1	0.2	1.2	<1	3
62	<5	<1	<20	89	0.9	<0.5	7	0.3	1.2	<1	<2
63	12	2	<20	81	1.7	<0.5	3	0.3	1.6	<1	<2
64	6	<1	<38	130	<0.5	<0.5	<1	0.5	<0.5	<1	5
65	<5	<1	<21	<50	2.4	<0.5	<1	0.3	1.6	<1	2
66	5	<1	<39	<50	1.1	<0.5	<1	<0.1	<0.5	<1	<2
67	11	2	<22	68	1.4	<0.5	<1	<0.1	<0.5	<1	3

Table 7. Chemistry of uncommon trace elements—Continued

[All analyses by neutron activation in ppm by weight; <, less than; Au as ppb by weight; Se<3 ppm, Ag<5 ppm, Sn<100 ppm, Ir<5 ppb, and Hg<1 ppm]

Sample site number	Cr	Co	Ni	Zn	As	Br	Mo	Sb	Ta	W	Au
68	5	<1	<22	<50	0.9	<0.5	<1	0.3	<0.5	<1	2
69	8	<1	<21	<50	<0.5	<0.5	<1	0.3	<0.5	<1	<2
70	6	2	<20	87	<0.5	<0.5	2	0.2	<0.5	<1	2
71	<5	2	<20	78	<0.5	<0.5	<1	0.3	1.1	<1	<2
72	<5	<1	<26	<50	4.5	<0.5	4	0.5	<0.5	<1	<2
73	<5	4	<33	93	<0.5	<0.5	<1	<0.1	<0.5	<1	3
74	8	<1	160	60	3.5	<0.5	2	0.3	<0.5	<1	<2
75	9	1	<20	99	1.2	<0.5	<1	0.3	<0.5	<1	3
76	8	<1	<35	<50	<0.5	<0.5	<1	0.3	1.8	<1	3
77	14	<1	<20	98	<0.5	<0.5	4	0.4	1.8	<1	<2
78	7	2	<20	82	<0.5	<0.5	3	<0.1	<0.5	<1	<2
79	19	2	<20	62	1.4	<0.5	5	<0.1	<0.5	<1	6
80	5	<1	<32	<50	<0.5	<0.5	<1	0.3	<0.5	<1	<2
81	6	2	120	<50	<0.5	<0.5	<1	0.4	<0.5	<1	<2
82	16	<1	180	86	<0.5	<0.5	2	<0.1	<0.5	<1	5
83	<5	<1	<20	96	3.7	<0.5	5	0.4	1.2	2	4
84	6	<1	<32	<50	2.4	<0.5	<1	<0.1	<0.5	<1	<2
85	<5	<1	<29	<50	2.2	<0.5	<1	0.3	2.7	<1	2
86	11	<1	<20	80	3.1	0.7	<1	0.4	0.8	<1	<2
87	7	<1	<28	<50	<0.5	<0.5	<1	<0.1	<0.5	3	<2
88	<5	1	<20	58	6.5	<0.5	<1	0.7	1.0	<1	<2
89	7	1	<20	100	0.9	<0.5	<1	<0.1	1.1	110	<2
90	7	<1	<35	91	<0.5	<0.5	2	<0.1	<0.5	<1	<2
91	11	2	<20	63	<0.5	<0.5	<1	0.3	<0.5	<1	<2
92	<5	3	<30	99	2.5	<0.5	<1	<0.1	<0.5	<1	<2
93	<5	<1	<33	120	2.4	<0.5	<1	0.4	1.7	<1	<2
94	<5	<1	<32	99	2.2	<0.5	9	0.3	<0.5	<1	<2
95	7	<1	<30	90	2.8	<0.5	<1	<0.1	<0.5	<1	<2
96	<5	<1	<31	<50	2.1	<0.5	<1	0.3	<0.5	<1	<2
97	9	<1	<32	<50	2.7	<0.5	<1	0.9	<0.5	<1	<2
98	7	<1	<22	63	7.3	1.8	<1	0.7	<0.5	<1	<2
99	8	2	<26	<50	1.9	<0.5	6	<0.1	2.4	<1	<2
100	6	3	<31	110	<0.5	<0.5	3	0.4	<0.5	<1	<2
101	10	<1	<27	51	<0.5	<0.5	<1	0.4	<0.5	<1	<2

Table 7. Chemistry of uncommon trace elements—Continued

[All analyses by neutron activation in ppm by weight; <, less than; Au as ppb by weight; Se<3 ppm, Ag<5 ppm, Sn<100 ppm, Ir<5 ppb, and Hg<1 ppm]

Sample site number	Cr	Co	Ni	Zn	As	Br	Mo	Sb	Ta	W	Au
102	12	<1	<24	80	3.9	<0.5	<1	0.3	1.7	<1	<2
103	10	<1	120	<50	3.5	<0.5	<1	0.3	1.2	<1	<2
104	15	<1	<21	<50	3.4	<0.5	<1	0.5	<0.5	<1	<2
105	6	<1	<23	52	3.0	<0.5	<1	0.3	<0.5	<1	<2
106	7	<1	<21	64	3.7	<0.5	2	0.3	1.9	<1	<2
107	10	<1	<23	70	3.4	1.4	<1	0.3	1.6	<1	<2
108	7	<1	<22	<50	3.9	<0.5˙	<1	0.3	1.5	<1	<2
110	6	<1	<21	73	7.3	<0.5	5	0.3	1.4	<1	<2
111	7	<1	<27	100	2.5	<0.5	<1	0.3	1.1	<1	<2
112	9	<1	<27	79	2.9	<0.5	<1	0.3	<0.5	<1	<2
113	<5	2	<27	67	1.9	<0.5	<1	<0.1	<0.5	<1	<2
114	7	<1	<22	65	1.9	<0.5	<1	0.4	1.2	<1	<2
115	13	2	<24	80	3.5	<0.5	<1	<0.1	<0.5	<1	<2
116	11	<1	120	<50	2.4	<0.5	<1	<0.1	<0.5	<1	<2
117	11	<1	<22	<50	2.4	<0.5	<1	0.2	1.7	3	<2
118	<5	3	<25	<50	3.4	<0.5	<1	<0.1	<0.5	<1	<2
119	<5	1	<22	90	4.9	<0.5	<1	0.4	1.4	<1	<2
120	10	<1	<26	68	3.4	<0.5	<1	0.3	<0.5	<1	<2
121	<5	<1	<27	<50	<0.5	<0.5	<1	0.5	<0.5	<1	<2
122	5	<1	<25	<50	2.6	<0.5	<1	<0.1	1.6	<1	3
123	9	<1	<28	110	3.4	<0.5	<1	0.4	<0.5	<1	<2
124	7	2	<20	76	7.5	2.1	4	0.6	1.2	<1	<2
125	10	<1	<20	90	2.7	<0.5	<1	0.2	1.5	<1	<2
126	<5	<1	<20	120	10.0	1.5	<1	0.4	<0.5	29	<2
127	14	<1	<20	<50	3.1	<0.5	<1	0.2	<0.5	<1	<2
128	10	1	<21	57	1.8	<0.5	<1	0.3	0.7	<1	<2
129	5	1	<20	94	<0.5	<0.5	3	0.2	1.5	<1	<2
130	7	1	<23	97	<0.5	<0.5	3	<0.1	1.0	<1	<2
131	7	3	<22	58	1.9	<0.5	3	0.2	<0.5	<1	2
132	5	2	<27	110	<0.5	<0.5	3	<0.1	1.3	<1	<2
133	<5	<1	<26	67	1.4	<0.5	<1	0.2	<0.5	<1	<2
134	9	<1	<33	100	<0.5	<0.5	<1	<0.1	1.8	<1	5
135	10	<1	<24	67	1.4	<0.5	<1	<0.1	<0.5	<1	<2
136	6	<1	<22	94	1.4	<0.5	4	<0.1	<0.5	<1	4

Table 7. Chemistry of uncommon trace elements—Continued

[All analyses by neutron activation in ppm by weight; <, less than; Au as ppb by weight; Se<3 ppm, Ag<5 ppm, Sn<100 ppm, Ir<5 ppb, and Hg<1 ppm]

Sample site number	Cr	Co	Ni	Zn	As	Br	Mo	Sb	Ta	W	Au
137	8	<1	<22	<50	<0.5	<0.5	<1	<0.1	<0.5	<1	4
138	<5	3	<22	<50	1.1	<0.5	4	0.3	<0.5	<1	4
139	8	<1	<21	<50	2.2	<0.5	3	0.3	<0.5	<1	4
140	14	<1	<21	74	1.5	<0.5	4	<0.1	<0.5	<1	<2
141	15	2	<22	<50	<0.5	<0.5	<1	0.2	<0.5	<1	<2
142	<5	<1	<20	71	1.6	1.6	<1	0.3	<0.5	<1	<2
143	10	<1	120	<50	1.2	<0.5	3	0.6	<0.5	<1	<2
144	9	<1	<20	74	2.7	<0.5	3	0.3	<0.5	<1	<2
145	8	<1	<20	<50	3.4	<0.5	<1	0.7	<0.5	<1	4
146	12	<1	<22	99	1.8	<0.5	<1	0.5	<0.5	<1	<2
147	<5	2	<21	<50	1.4	<0.5	3	<0.1	<0.5	<1	3
148	11	1	<20	73	1.6	<0.5	<1	0.2	<0.5	<1	<2
149	7	<1	<20	85	1.1	<0.5	<1	0.2	<0.5	<1	4
150	11	<1	<20	<50	<0.5	<0.5	2	<0.1	<0.5	<1	4
151	<5	<1	<20	77	<0.5	<0.5	<1	0.3	<0.5	<1	<2
152	12	<1	<20	75	<0.5	<0.5	4	0.3	<0.5	<1	<2
153	10	<1	<20	68	1.7	<0.5	<1	0.2	<0.5	<1	<2
154	7	<1	<20	<50	<0.5	<0.5	<1	<0.1	<0.5	<1	4
155	11	<1	<20	<50	<0.5	<0.5	<1	0.2	1.2	1	4
156	<5	<1	<20	78	1.0	<0.5	3	<0.1	<0.5	<1	4
157	12	<1	<31	<50	2.8	<0.5	6	0.4	<0.5	<1	<2
158	9	<1	<32	<50	3.3	<0.5	5	0.3	1.7	<1	<2
159	26	3	<32	110	4.6	<0.5	<1	0.3	<0.5	<1	<2

the Tiva Canyon Tuff are devitrified, contain biotite phenocrysts, and have vapor-phase minerals lining the pumice cavities (Singer and others, 1994). High-temperature devitrification of glass shards prevented subsequent low-temperature glass hydration. However, post-emplacement recrystallization of the tuffs and alteration by deuteric fluids would have resulted in slight and variable enrichments in ^{18}O, as proposed for some of the samples from the Solitario Canyon section. Deuteric alteration would have little effect on the distribution of most other elements and would be enhanced in zones that cooled slowly. The lack of correlations between δ^{18}O values and other elements, fault zones, or specific areas are further evidence that increases in ^{18}O in the upper cliff and caprock samples are unrelated to specific fluid events other than those associated with emplacement of the unit. The absence of any low δ^{18}O values indicates that hydrothermal alteration by meteoric waters, either during or after emplacement, was minimal (Taylor, 1974).

The addition of small quantities of low-temperature carbonate and silica, which have high δ^{18}O values in excess of +19 ‰ (Vaniman and Whelan, 1994), to the upper cliff and caprock samples cannot be totally discounted as a process that elevates the whole-rock δ^{18}O values. However, there is no cor-relation between δ^{18}O values and calcium contents as would be expected if pedogenic calcite were the source of the high δ^{18}O values. Small quantities of pedogenic carbonate may have resulted in elevation of the original calcium contents, but the effect on whole-rock δ^{18}O values is minimal as discussed above for the samples from the Solitario Canyon section. The addi-tion of low-temperature silica is more difficult to assess, although none was observed during petro-graphic examination. Late-stage fracture coatings of chalcedony are present in areas of the upper cliff zone, but these areas were avoided during sampling. The δ^{18}O value of one such coating from the sample at map location 108 (fig. 2) is +28 ‰. The adjacent tuff has a value of +9.4 ‰, indicating that infiltration of late-stage silica, if present, is minimal.

CONCLUSIONS

Most of the variations in the chemical composi-tions of the high-silica rhyolite and quartz latite from the Tiva Canyon Tuff reflect magmatic processes. Only elements such as sodium, calcium, and uranium that can be easily mobilized by low-temperature fluids appear to have been affected by post-eruptive fluid-rock interactions. However, these interactions are restricted to deuteric alteration, in which magmatic fluids precipitated silica and feldspar, and to low-temperature alteration, in which silica and carbonate were precipitated from meteoric waters. None of the samples of the Tiva Canyon Tuff have high concentra-tions of trace elements such as arsenic, silver, mercury, or gold that would indicate hydrothermal alteration or epithermal mineralization.

The δ^{18}O values of whole-rock samples of the Tiva Canyon Tuff range from +6.9 to +11.8 ‰. Most are higher than the presumed magmatic values of +6 to +8 ‰, but none are lower. Whole-rock δ^{18}O values have been elevated primarily as a result of deuteric alteration during cooling of the ash-flow unit. Minor addition of carbonate and silica from low-temperature meteoric waters and low-temperature hydration of vol-canic glass, where not devitrified, also may have con-tributed to the high δ^{18}O values in some samples.

Most significant from a mineral resources per-spective is the lack of similarity between both oxygen isotopic compositions and pathfinder elements in proximal mineralized areas and those measured in this study. O'Neil and Silberman (1974) reported δ^{18}O values less than 5 permil for silicate minerals from epithermal gold and silver deposits in Nevada and attributed such low values to precipitation from hydrothermal meteoric waters. Quartz from the Bullfrog gold mine near Beatty and the Goldfield gold mine near Tonopah have δ^{18}O values of 5.2 and -1.2 permil, respectively. These values are signifi-cantly lower than any of those measured in samples from the Tiva Canyon Tuff, indicating an absence of hydrothermal alteration and significant epithermal mineralization in this part of the volcanic section at Yucca Mountain.

REFERENCES CITED

Benson, L.V., and McKinley, P.W., 1985, Chemical composition of ground water in the Yucca Mountain area, Nevada, 1971–1984: U.S. Geological Survey Open-File Report 85-484, 10 p.

Broxton, D.E., Warren, R.G., and Byers, F.M., 1989, Chemical and mineralogic trends within the Timber Mountain-Oasis Valley caldera complex, Nevada—Evidence for multiple cycles of chemical evolution in a long-lived silicic magma system: Journal of Geophysical Research, v. 94, no. B5, p. 5961–5985.

Buesch, D.C., Spengler, R.W., Moyer, T., and Geslin, J., 1996, Revised stratigraphic nomenclature and macroscopic identification of lithostratigraphic units of the Paintbrush Group exposed at Yucca Mountain, Nevada: U.S. Geological Survey Open-File Report 94-469, 45 p.

Castor, S.B., Feldman, S.C., and Tingley, J.V., 1990, Mineral evaluation of the Yucca Mountain addition, Nye County, Nevada: Nevada Bureau of Mines and Geology Open-File Report 90-4, 80 p.

Connors, K.A., Noble, D.C., Bussey, S.D., and Weiss, S.I., 1993, Initial gold contents of silicic volcanic rocks—Bearing on the behavior of gold in magmatic systems: Geology, v. 21, no. 10, p. 937–940.

Cornwall, H.R., 1972, Geology and mineral deposits of southern Nye County, Nevada: Nevada Bureau of Mines and Geology Bulletin 77, 49 p.

Criss, R.E., and Taylor, H.P., Jr., 1986, Meteoric-hydrothermal systems, in Valley, J.W., Taylor, H.P., Jr., and O'Neil, J.R., eds., Stable isotopes in high temperature geological processes: Mineralogical Society of America, Reviews in Mineralogy, v. 16, p. 373–424.

Ewers, G.R., Mackenzie, D.E., Wyborn, D., Oversby, B.S., McPhie, J., and Andrew, A.S., 1994, Regional ^{18}O depletions in igneous rocks from the northern Drummond Basin, Queensland, Australia, and their implications for epithermal gold mineralization: Economic Geology, v. 89, no. 3, p. 662–673.

Farmer, G.L., Broxton, D.E., Warren, R.G., and Pickthorn, W., 1991, Nd, Sr, and O isotopic variations in the metaluminous ash-flow tuffs and related volcanic rocks at the Timber Mountain/Oasis Valley caldera complex, SW Nevada—Implications for the origin of large-volume silicic magma bodies: Contributions to Mineralogy and Petrology, v. 109, no. 1, p. 53–68.

Ferriz, H., and Mahood, G.A., 1987, Strong compositional zonation in a silicic magmatic system—Los Humeros, Mexican neovolcanic belt: Journal of Petrology, v. 28, no. 1–3, p. 171–209.

Flood, T.P., Vogel, T.A., and Schuraytz, B.C., 1989, Chemical evolution of a magmatic system—The Paintbrush Tuff, southwest Nevada volcanic field: Journal of Geophysical Research, v. 94, no. B5, p. 5943–5960.

Friedman, I., and Smith, R.L., 1960, A new dating method using obsidian—Part I, the development of the method: American Antiquity, v. 25, p. 476–522.

Greybeck, J.D., and Wallace, A.B., 1991, Gold mineralization at Fluorspar Canyon near Beatty, Nye County, Nevada, in Raines, G.L., Lisle, R.E., Schafer, R.W., and Wilkinson, W.H., eds., Geology and ore deposits of the Great Basin: Reno, Geological Society of Nevada, p. 935–946.

Grow, J.A., Barker, C.E., and Harris, A.G., 1994, Oil and gas exploration near Yucca Mountain, southern Nevada, in High Level Radioactive Waste Management, 5th [Proceedings]: La Grange Park, Ill., American Nuclear Society, p. 1298–1315.

Halliday, A.N., Fallick, A.E., Hutchinson, J., and Hildreth, W., 1984, A Nd, Sr and O isotopic investigation into the causes of chemical and isotopic zonation in the Bishop Tuff, California: Earth and Planetary Science Letters, v. 68, no. 3, p. 379–391.

Hildreth, W., 1979, The Bishop Tuff—Evidence for the origin of compositional zonation in silicic magma chambers: Geological Society of America Special Paper 180, p. 43–75.

———1981, Gradients in silicic magma chambers—Implications for lithospheric magmatism: Journal of Geophysical Research, v. 86, no. 11–12, p. 10153–10192.

Hildreth, W., Christiansen, R.L., and O'Neil, J.R., 1984, Catastrophic isotopic modification of rhyolitic magma at times of caldera subsidence, Yellowstone Plateau volcanic field: Journal of Geophysical Research, v. 89, no. B10, p. 8339–8369.

Hildreth, W., and Michael, P.J., 1983, Comment and reply on "Chemical differentiation of the Bishop Tuff and other high-silica magmas through crystallization processes": Geology, v. 11, no. 10, p. 622–624.

Levinson, A.A., 1980, Introduction to exploration geochemistry: Wilmette, Ill., Applied Publishing, 924 p.

Lipman, P.W., Christiansen, R.L., and O'Connor, J.T., 1966, A compositionally zoned ash-flow sheet in southern Nevada: U.S. Geological Survey Open-File Report 524-F, p. F1–F47.

Lipman, P.W., and Friedman, I., 1975, Interaction of meteoric water with magma—An oxygen-isotope study of ash-flow sheets from southern Nevada: Geological Society of America Bulletin, v. 86, no. 5, p. 695–702.

McCulloch, M.T., Kyser, T.K., Woodhead, J.D., and Kinsley, L., 1994, Pb-Sr-Nd-O isotopic constraints on the origin of rhyolites from the Taupo volcanic zone of New Zealand—Evidence for assimilation followed by

fractionation from basalt: Contributions to Mineralogy and Petrology, v. 115, no. 1, p. 303–312.

Neymark, L.A., Marshall, B.D., Kwak, L.M., Futa, K., and Mahan, S.A., 1995, Geochemical and Pb, Sr, and O isotopic study of the Tiva Canyon Tuff and Topopah Spring Tuff in the vicinity of Yucca Mountain, Nye County, Nevada: U.S. Geological Survey Open-File Report 95-134, 17 p.

O'Neil, J.R., and Silberman, M.L., 1974, Stable isotope relations in epithermal Au-Ag deposits: Economic Geology, v. 69, no. 6, p. 902–909.

O'Neill, J.M., Whitney, J.W., and Hudson, M.R., 1992, Photogeologic and kinematic analysis of lineaments at Yucca Mountain, Nevada—Implications for strike-slip faulting and oroclinal bending: U.S. Geological Survey Open-File Report 91-623, 24 p.

Ohmoto, H., 1986, Stable isotope geochemistry of ore deposits, in Valley, J.W., Taylor, H.P., Jr., and O'Neil, J.R., eds., Stable isotopes in high temperature geological processes: Mineralogical Society of America, Reviews in Mineralogy, v. 16, p. 491–559.

Pearce, J.A., and Cann, J.R., 1973, Tectonic setting of basic volcanic rocks determined using trace element analysis: Earth and Planetary Science Letters, v. 19, no. 2, p. 290–300.

Peterman, Z.E., and Futa, K., 1996, Geochemistry of core samples of the Tiva Canyon Tuff from drill hole UE-25 NRG#3, Yucca Mountain, Nevada: U.S. Geological Survey Open-File Report, 19 p.

Peterman, Z.E., Widmann, B.L., Marshall, B.D., Aleinikoff, J.N., Futa, K., and Mahan, S.A., 1994, Isotopic tracers of gold deposition in Paleozoic limestones, southern Nevada, in High Level Radioactive Waste Management, 5th [Proceedings]: La Grange Park, Ill., American Nuclear Society, p. 1316–1323.

Ransome, F.L., 1907, Preliminary account of Goldfield, Bullfrog, and other mining districts in southern Nevada: U.S. Geological Survey Bulletin 303, 98 p.

——1910, Geology and ore deposits of the Bullfrog District, Nevada: U.S. Geological Survey Bulletin 407, 130 p.

Romberger, S.B., 1988, Disseminated gold deposits, in Roberts, R.G., and Sheahan, P.A., eds., Ore Deposit Models: Geoscience Canada Reprint Series, v. 3, p. 21–30.

——1993, A model for bonanza gold deposits, in Sheahan, P.A., and Cherry, M.E., eds., Ore Deposit Models: Geoscience Canada Reprint Series, v. 6, p. 77–86.

Ross, C.S., and Smith, R.L., 1955, Water and other volatiles in volcanic glasses: American Mineralogist, v. 40, no. 11–12, p. 1071–1089.

——1961, Ash-flow tuffs—Their origin and geologic relations and identification: U.S. Geological Survey Open-File Report 366, 81 p.

Sawyer, D.A., Fleck, R.J., Lanphere, M.A., Warren, R.G., Broxton, D.E., and Hudson, M.R., 1994, Episodic volcanism in the Miocene southwest Nevada volcanic field—Stratigraphic revisions, $^{40}Ar/^{39}Ar$ geochronologic framework, and implications for magmatic evolution: Geological Society of America Bulletin, v. 106, no. 10, p. 1304–1318.

Schuraytz, B.C., Vogel, T.A., and Younker, L.W., 1989, Evidence for dynamic withdrawal from a layered magma body—The Topopah Spring Tuff, southwestern Nevada: Journal of Geophysical Research, v. 94, no. B5, p. 5925–5942.

Scott, R.B., and Bonk, J., 1984, Preliminary geologic map of Yucca Mountain, Nye County, Nevada, with geologic sections: U.S. Geological Survey Open-File Report 84-494, scale 1:12,000.

Singer, F.R., Byers, F.M., Jr., Widmann, B.L., and Dickerson, R.P., 1994, Petrographic and geochemical characteristics of a section through the Tiva Canyon Tuff at Antler Ridge, Yucca Mountain, Nevada, in High Level Radioactive Waste Management, 5th [Proceedings]: La Grange Park, Ill., American Nuclear Society, p. 1869–1879.

Smith, R.L., 1960, Zones and zonal variations in welded ash flows: U.S. Geological Survey Open-File Report 354-F, p. 149–159.

Spengler, R.W., and Fox K.R., Jr., 1989, Stratigraphic and structural framework of Yucca Mountain, Nevada: Radioactive Waste Management and the Nuclear Fuel Cycle, v. 13, p. 21–36.

Stuckless, J.S., and O'Neil, J.R., 1973, Petrogenesis of the Superstition-Superior volcanic area as inferred from strontium- and oxygen-isotope studies: Geological Society of America Bulletin, v. 84, no. 6, p. 1987–1998.

Szabo, B.J., and Kyser, T.K., 1990, Ages and stable isotope compositions of secondary calcite and opal in drill cores from Tertiary volcanic rocks of the Yucca Mountain area, Nevada: Geological Society of America Bulletin, v. 102, no. 12, p. 1714–1719.

Taylor, B.E., 1991, Degassing of Obsidian Dome rhyolite, Inyo volcanic chain, California, in Taylor, H.P., Jr., O'Neil, J.R., and Kaplan, I.R., eds., Stable isotope geochemistry—A tribute to Samuel Epstein: San Antonio, The Geochemical Society, p. 339–353.

Taylor, H.P., Jr., 1968, The oxygen isotope geochemistry of igneous rocks: Contributions to Mineralogy and Petrology, v. 19, no. 1, p. 1–71.

———1974, The application of oxygen and hydrogen isotope studies to problems of hydrothermal alteration and ore deposition: Economic Geology, v. 69, no. 6, p. 843–883.

———1986, Igneous rocks—II. Isotopic case studies of circumpacific magmatism, *in* Valley, J.W., Taylor, H.P., Jr., and O'Neil, J.R., eds., Stable isotopes in high temperature geological processes: Mineralogical Society of America, Reviews in Mineralogy, v. 16, p. 273–317.

Taylor, H.P., Jr., and Epstein, S., 1962, Relationship between $^{18}O/^{16}O$ ratios in coexisting minerals of igneous and metamorphic rocks: Geological Society of America Bulletin, v. 73, no. 4, p. 461–480.

Taylor, H.P., Jr., and Sheppard, S.M.F., 1986, Igneous rocks I. Processes of isotopic fractionation and isotope systematics, *in* Valley, J.W., Taylor, H.P., Jr., and O'Neil, J.R., eds., Stable isotopes in high temperature geological processes: Mineralogical Society of America, Reviews in Mineralogy, v. 16, p. 227–272.

Taylor, S.R., and McClennan, S.M., 1985, The continental crust—Its composition and evolution: Palo Alto, Blackwell Scientific, 312 p.

U.S. Department of Energy, 1988, Site characterization plan, Yucca Mountain site, Nevada Research and Development Area, Nevada: U.S. Department of Energy Report DOE RW/0199, 8 vols.

Valley, J.W., Taylor, H.P., Jr., and O'Neil, J.R., eds., 1986, Stable isotopes in high temperature geological processes: Reviews in Mineralogy, v. 16, 570 p.

Vaniman, D.T., and Whelan, J.F., 1994, Inferences of paleoenvironment from petrographic, chemical and stable-isotope studies of calcretes and fracture calcites, *in* High Level Radioactive Waste Management, 5th [Proceedings]: La Grange Park, Ill., American Nuclear Society, p. 2730–2737.

Weiss, S.I., Noble, D.C., and Larson, L.T., 1994, Potential for undiscovered mineral deposits at Yucca Mountain, NV—Host rocks, timing and spatial distribution of nearby mineralization [abs.]: Geological Society of America Abstracts with Programs, v. 26, no. 7, p. A311.

Winograd, I.J., Szabo, B.J., Coplen, T.B., and Riggs, A.C., 1988, A 250,000-year climatic from Great Basin vein calcite?implications for Milankovich theory: Science, v. 242, p. 1275–1280.

Younker, J.L., and others, 1992, Report of early site suitability evaluation of the potential repository site at Yucca Mountain, Nevada: Science Applications International Corporation Report SAIC-91/8000, p. 2-121–2-145.